Full title: Identification of novel plasma proteomic biomarkers of Dupuytren Disease

Short title: Dupuytren plasma proteomic biomarkers

Blake Hummer[1¶], Paola Sebastiani[2,3&], Anastasia Leshchyk[4&], Anastasia Gurinovich[2,3&], Cecilie Bager[5&], Morten Karsdal[5&], Signe Nielsen[5&], Charles Eaton[1¶*]

[1] Dupuytren Research Group, West Palm Beach, Florida, United States of America

[2] Institute for Clinical Research and Health Policy Studies, Tufts Medical Center, Boston, Massachusetts, United States of America

[3] Department of Medicine, Tufts University, Boston, Massachusetts, United States of America

[4] Department of Medicine, Computational Biomedicine Section, Chobanian & Avedisian School of Medicine, Boston University, Boston, Massachusetts, United States of America

[5] Nordic Bioscience, Herlev, Denmark

* Corresponding Author

Email: c.eaton.md@dupuytrens.org (CE)

[¶] These authors contributed equally to this work.

[&] These authors also contributed equally to this work.

Abstract

Dupuytren Disease (DD) is a chronic progressive disease that can cause disabling hand deformities. The most common treatments have either high complication rates or high early recurrence rates. Dupuytren lacks a staging biomarker profile to inform the development of preventive therapeutics to improve long-term outcomes. This multi-omic study aimed to create a DD blood proteomic biomarker profile by comparing DD plasma with that of a healthy control group. We measured circulating collagen metabolism peptides and found normal Collagen I synthesis but impaired Collagen I degradation in DD. We measured 6995 serum protein aptamers and identified 68 proteins that showed statistically significant differences compared with the control group. We developed two Diagnostic Proteomic Risk Scores (DPRS) based on hypothesis-free and hypothesis-based analyses. In independent data, our hypothesis-free and hypothesis-based DPRS distinguished Dupuytren from control subjects with accuracies of 76.5% and 70.6%, respectively. Our hypothesis-based DPRS also distinguished DD subjects with different disease progression rates by age at their first corrective procedure (p=0.0018). This pilot study is the first to provide evidence to suggest that Collagen I accumulation in DD results from impaired degradation rather than increased collagen synthesis. It also describes novel DPRS that have potential use as diagnostic and staging biomarker panels for Dupuytren disease.

Introduction

Dupuytren disease (DD) is a progressive fibrotic condition that often results in finger deformities called Dupuytren contracture (DC). DD affects an estimated 10 million Americans. DC is associated with loss of productivity, higher healthcare costs, and a greater prevalence of benign diseases [1].

The greatest need in DD care is preventing DC progression and recurrence. As with other fibrotic diseases, developing preventive treatments requires a biomarker profile for staging and measuring therapeutic response. The authors have not found published reports with statistically significant evidence of preventing DC recurrence or a biomarker tool to develop such treatments. This pilot study aimed to develop preliminary data on a diagnostic blood biomarker profile of DD.

DC is a common outcome of DD. Of those diagnosed with DD at age 65, one in four men and one in eight women will require at least one corrective procedure over their lifetime [2]. The most common current treatments are palliative, often resulting in partial or temporary improvement [3]. Surgery for DC has a greater risk of major complications than other common elective hand operations [4-7], and recurrent DC is the most common diagnosis leading to elective finger amputation [8].

Genetic factors account for about 80% of the risk of developing DD [9]. Family history, age, and gender are strongly associated. A genetic risk score (GRS) based on 11 SNPs correlates with DD diagnosis [10], and a weighted GRS based on 26 SNPs correlates with post-procedure recurrence [11].

DD affects the palm skin, subcutaneous tissues, and fascia [12]. Early disease is cellular, with fibroblasts, myofibroblasts, and perivascular clusters of myofibroblasts, pericytes, and

mononuclear immune cells [13]. Early changes include local variations of immune [13], hematopoietic, and mesenchymal cell markers [12], cytokines, signaling factors [14], and extracellular matrix components [15, 16]. Progression transforms tissues into nearly acellular, densely packed collagen.

Physical changes are the basis for DD diagnosis, staging, and treatment, but physical findings do not predict progression [17]. There are no standard noninvasive tests of DD biological activity. Biopsy is problematic because it can trigger disease activity and progression. Blood remains the most promising source for a disease activity profile.

Materials and methods

Study Approval

The Institutional Review Board Ascension Via Christi Hospitals, Wichita, Inc., approved this study and the associated informed consent form. Written informed consent was obtained from all participants before their participation. This written informed consent included a description of the use of the photographs/ images to be reviewed for study entry. The records of these signed informed consents are held on file by the investigators in accordance with PLOS policies. All samples remained blinded throughout the processing and data collection in the laboratories. All methods were performed in accordance with relevant guidelines, regulations, and the Declaration of Helsinki.

Subjects

We selected disease cohort subjects from the International Dupuytren Database (IDDB), a patient-reported registry developed by the Dupuytren Research Group (DRG) in collaboration with the National Databank of Rheumatic Diseases (NDB). Control subjects were enrolled by

word of mouth and from the NDB database (https://dupuytrens.org/enroll-in-the- iddb-2/). Study candidate subjects were identified on December 3, 2019, using the entry criteria described below. We excluded minors from the study. Our study involved male and female subjects. Sex was considered a biological variable. While we controlled for sex differences, we did not stratify by sex due to limited sample sizes. The authors had no access to information that could identify individual participants during or after data collection. All subjects met the entry criteria, and each subject submitted a signed physical Informed Consent Form by postal mail. Recruitment started on December 13, 2019, and ended on May 3, 2021.

Entry criteria

The DD cohort met criteria based on clinical evidence of DD with strong traditional predictors of recurrent deformity after a corrective procedure: age of disease onset younger than 50; two or more first-degree relatives with DD; current DD nodules; three or more separate locations of DD, or two palm locations and Ledderhose disease (a related disorder). Control cohort subjects were healthy individuals with no clinical evidence of DD, no personal history of DD or Ledderhose disease, and no family history of DD.

We confirmed study eligibility by requiring candidates to upload recent images of the palmar and dorsal sides of each hand. The Principal Investigator/senior author confirmed the entry criteria and reviewed images to confirm clinical evidence of active DD in the disease cohort and the absence of these findings in the control cohort.

Blood Sample Collection

The study used a mobile phlebotomy service (Phlebotek Solutions Corporation, Fort Lauderdale, FL) to collect blood specimens. Once confirmed that the subject met all study entry

criteria, they were contacted by DRG and later by Phlebotek to schedule their blood draw. The phlebotomist visited the subjects in their homes and collected two tubes of blood. The last 16 blood draws included a third 2.5ml PAXgene tube collection for additional genomic testing.

Processing of the EDTA tubes for proteomic testing was standardized. Immediately following collection, blood samples were centrifuged for 15 minutes at 2000 g to generate plasma. The plasma was harvested from the top of the container and pooled before aliquoting into storage cryotubes. The last 500 µL of plasma was discarded to avoid contamination with platelets. Samples were immediately packaged for shipping on dry ice.

Number of subjects

One hundred subjects were planned (50 DD/50 Control). This number was a practical consideration, given the limited number of potential participants enrolled in the International Dupuytren Data Bank who met all disease cohort entry criteria. Blood collection launched in February 2020, just as the COVID pandemic began. Due to COVID-related issues, we amended the protocol to enroll 50 subjects. Forty-seven subjects were enrolled;46 subjects had samples drawn. One sample was disqualified due to failed shipping refrigeration. Mass spectrometry (Bioproximity, Manassas, VA) was performed on samples from the remaining 45 subjects (25 DD, 20 Control). Twenty-seven subjects (13 DD, 14 control) had second blood samples drawn 6 to 14 months after their first draw for mass spectrometry testing by a second lab (MacCoss Lab, Seattle, WA). Additional proteomic testing was conducted on remaining aliquots: 1) n= 27 redrawn samples had ELISA tests for collagen metabolites (Nordic Bioscience, Herlev, DK); 2) n= 72 from both initial and redraw specimens had Aptamer-based testing (SomaLogic, Boulder, CO). S1 Fig outlines the distribution of samples and laboratories.

Blinding

All subjects were assigned and identified by participant numbers. Investigators were blinded to the sample group allocation. All samples remained blinded throughout the processing and data collection in the laboratories.

Assays

No laboratory protocols were conducted in-house.

Nordic Bioscience collagen markers

Circulating collagen synthesis and degradation markers were measured using proprietary assays [18]. Synthesis biomarkers included collagens I (PRO-C1), II (PRO-C2), III (PRO-C3), IV (PRO-C4), V (PRO-C5), VI (PRO-C6), VII (PRO-C7), and IX (PRO-C9). Circulating degradation markers were measured for collagens I (C1M), II (CALC2, C2M), III (C3M, CTX-III), IV (C4M), VI (C6M), and VII (C7M). All biomarkers were assessed by competitive ELISAs and validated to measure in human plasma samples. The inter- and intra-assay coefficients of variation were >15% and 10%, respectively, for all assays.

Mass spectrometry

A novel untargeted proteomics assay using large-scale liquid chromatography-tandem mass spectrometry (LC-MS/MS) with data-independent acquisition (DIA) was used to collect proteomic data. Each sample (10 µl plasma), following tryptic digestion, was diluted 50:50 by the addition of 4% sodium dodecyl sulfate (SDS) buffer to a final concentration of ~2% SDS. Approximately 200 µg of protein was added to 96-well plates, and the remainder of the sample preparation was performed using the single-pot, solid-phase enhanced sample preparation for proteomics methodology (SP3) [19, 20]. The entire process of protein capture, reduction and alkylation, protein cleanup, digestion, and peptide cleanup was performed using a KingFisher

magnetic bead robot [20]. Peptides were reconstituted in HPLC starting aqueous buffer (5% acetonitrile and 0.1% formic acid) with analysis performed on the high-resolution quadrupole-orbitrap hybrid mass spectrometer (Exploris 480, Orbitrap Fusion Lumos, or Orbitrap Fusion Eclipse).

Data was acquired in a single, 2-hour LC-MS/MS run (90 min HPLC gradient) on a Thermo Quadrupole-Orbitrap mass spectrometer. Crucially, the DIA method comprehensively sampled all peptides between 400 and 1000 m/z using a repeated cycle of 75 MS/MS scans with an 8 m/z-wide isolation width. Using a multiplexing scheme based on staggering the isolation window in alternating cycles of MS/MS scans, the precursor selectivity of the resulting data was 4 m/z after computational demultiplexing [21]. From the resulting data, fragment ion chromatograms were extracted for any peptide precursor between 400 and 1000 m/z. To determine which peptides were confidently detected in each acquisition, the software tool EncyclopeDIA [22] was used to query the data using a reference chromatogram library generated from a prior analysis of the tissue. Chromatogram-based relative quantitation was then performed for each peptide detected. All measurements were made relative to a common reference. In the case of plasma, a common reference was a pooled standard from 400 age-matched samples from subjects who were both healthy and spanning the phenotypes being studied, processed in each sample batch. Within each 96-well plate, one copy of the common reference standard was placed in each row for a total of 8 copies per plate [23]. Before quantification, it was confirmed that peptides were stable during the time scale of the data collection, had a suitable linear response, and had suitable intra- and inter-data precision.

SomaScan

SomaLogic, Inc. (Boulder, CO, USA) performed proteomic analysis of the plasma samples using the SomaScan platform, which quantifies the presence of 6995 human proteins (secreted

proteins, extracellular domains, and intracellular proteins). These proteins are found in diverse biological groups such as receptors, kinases, cytokines, proteolytic enzymes and inhibitors, growth factors, protease inhibitors, hormones, and structural proteins [24]. Most of these proteins are involved in pathways related to signal transduction, stress response, immune processes, phosphorylation, proteolysis, cell adhesion, cell differentiation, and intracellular transport [25].

Proteins were measured using the Slow Off-Rate Modified Aptamer (SOMAmer)-based capture array, which uses chemically modified single-stranded DNA sequences capable of uniquely recognizing individual proteins via one or more binding sites. SOMAmers transform a protein signal to a nucleotide signal that is quantified using relative fluorescence on microarrays. Each SOMAmer array underwent validation for specificity, upper and lower limits of detection, and both intra- and inter-assay variability. Plasma dilutions (0.005%, 0.05%, and 20%) were applied to capture low-, medium-, and high-abundance proteins. Positive and negative controls were also positioned on the array to confirm if the experimental procedure was performed correctly.

After the hybridization step, the microarrays were washed and scanned using a laser scanner that excites the fluorescence of the fluorochrome used in the labeling step. The amount of the emitted signal is directly proportional to the amount of dye on the microarray. The scanner measured this quantity and created a digital image map of the position of each signal based on the location of its origin. Image analysis software generated a text file from this map describing the pixel intensity of the spot and the background. This information was processed, and a final value was generated that summarized the level of each detectable protein on the microarray.

Quality control analysis of the sample and SOMAmer levels involved SOMAmer control arrays on the microarray and calibration samples. Hybridization controls measured the sample-by-

sample variation in hybridization, while the median signal over all SOMAmer arrays measured the technical variability. The SomaScan measures were reported as relative fluorescence units (RFU) in a summary ADAT file.

Analysis and statistics

Nordic collagen marker analysis

Nordic collagen data turnover rates were calculated by performing ratios of the propeptide over the mature peptide (e.g., PRO-C1/ C1M). This ratio is an estimate of the formation/degradation of each collagen type and can be interpreted as a net gain of collagen/loss of collagen remodeling [18]. All comparisons were done using Student's T-test.

SomaScan analysis

A series of quality control and data cleaning steps was performed on the SomaScan proteomics data. All non-human proteins were excluded from the analyses. Samples that did not pass the default normalization acceptance criteria for all row scale factors were removed. All aptamers that did not pass the default quality control criteria across all plates/sets were filtered out. The data had no missing values, and the protein values were log-transformed. No further normalization was performed.

We identified differentially expressed aptamers using linear regression of each log-transformed protein as the outcome and disease status as the main predictor. We adjusted each analysis by age and sex. We analyzed all repeated measurements of each individual and employed generalized estimating equations to account for technical and biological variability using the gee package in R. Due to the high number of aptamers tested in the SomaScan assay (6995), we were at a statistical disadvantage when applying multiple corrections. Therefore, we calculated

adjusted p-values using Benjamini-Hochberg methods. Our SomaScan analyses report only proteins with statistically significant differences from the control at an FDR-adjusted p-value < 0.25.

Mass spectrometry analysis

For the MS protein data, all zeroes were replaced with NAs across samples, and protein values were log-transformed. The MS dataset was subset based on proteins that overlapped with the signature proteins associated with DD previously identified using the SomaScan proteomics data. We used a generalized estimation equation model to account for the repeated blood draws, adjusted by age and gender.

Proteomic Risk Score calculations

To prepare the data for the Diagnostic Proteomic Risk Score (DPRS) calculation, we first removed all highly correlated proteins (Pearson correlation > 0.8). 3369 out of 6995 aptamers were highly correlated and were excluded from the DPRS calculation. The DPRS calculation contained the following two steps. First, we fit a logistic regression for each protein, with disease status (i.e., case or control) as the outcome variable, adjusted for age and gender. We used a generalized estimation equation model for repeated measurements of two independent blood draws. We included the same subject's repeated measurements and used the generalized estimation equations model with the gee R package [26] to estimate the regression coefficients. Next, the DPRS was computed using summary statistics from each regression model. Only the proteins with statistically significant differences from control at an FDR-adjusted p-value < 0.25 were included in the score calculation. The DPRS was calculated by summing the beta estimated effect for all significant proteins, each multiplied by normalized protein abundance and divided by its standard error. Finally, we fit a logistic regression to examine the association

of the computed DPRS with DD onset. We split the dataset into training (75%) and testing sets utilizing the caret R package for a leave-one-out cross-validation approach for model fitting and assessment (25%) sets [27]. We used R version 4.2.1 for all analyses.

Pathway analysis

STRING (12.0) is a web tool that provides and illustrates protein-protein interactions and networks [28]. STRING integrates evidence from public databases, including genomic context, high-throughput and biochemical interaction experiments, known protein complexes, computational predictions, and text mining from scientific literature. Given a list of gene names, STRING constructs protein-protein interaction networks in which each gene is a node, with edges representing predicted functional associations.

Networks were generated using the whole genome as the statistical background, and interaction sources included text mining, experiments, databases, co-expression, neighborhood, gene fusions, and co-occurrence. Interaction scores were computed by combining the probabilities across all evidence channels and correcting for the probability of observing an interaction by chance. All nodes and interactions were computed with a required medium confidence interaction score (0.400) and an FDR<=0.05.

Results

Plasma collagen metabolites in DD

Collagen synthesis and degradation processes release protein fragments specific to the process, collagen type, and enzyme involved. The ratio of synthesis to degradation-related fragments correlates with net accumulation or loss of that collagen type. We evaluated plasma

markers of collagen synthesis and degradation using a competitive ELISA (Nordic Biosciences; Herlev, Denmark) and calculated collagen synthesis-to-degradation ratios [18].

We measured markers of types I, II, III, IV, V, VI, VII, and IX collagen metabolism in blood from a cohort of healthy controls (n = 14) and subjects with DD (n = 13). We found significantly lower levels of markers of Collagen I degradation (C1M; Fig 1A, p = 0.004), Collagen V synthesis (Pro-C5; Fig 1B, p = 0.046), and Collagen VII synthesis (Pro-C7; Fig 1C, p = 0.048) in the DD cohort compared to the control group. The remaining collagen biomarkers did not show significant differences between the disease and control groups (Table 1).

Fig 1. Differential production of Dupuytren vs. control collagen metabolism markers. A) Collagen I degradation marker C1M. B) Collagen I synthesis to degradation marker ratio Pro-C1/C1M. C) Collagen V synthesis marker Pro-C5. D) Collagen VII synthesis marker Pro-C7. * p-value <0.05, **p-value <0.005.

Table 1. Collagen epitope markers and findings.

Assay	D/C	Description	Represents	p-value	SE	FC (D/C)
PRO_C1_HP	ns	Internal epitope in the N-terminal propeptide of type I collagen	Col I Synthesis	0.9437	C 10.99 D 11.89	0.93
C1M_HP	Down**	MMP-generated fragment of the a1 chain of type I collagen	Col I Degradation	0.0036	C 5.25 D 4.30	0.73
PRO-C2_HP	ns	N-terminal fragment of type IIB procollagen	Col II Synthesis	0.7808	C 1.45 D 3.11	1.01
CALC2	ND	C-terminal propeptide of type II collagen	Col II Synthesis	NA	NA	NA
C2M_HP	ns	MMP-generated fragment of type II collagen	Col II Degradation	0.1607	C 1.52 D 1.16	1.29
PRO-	ns	N-terminal propeptide of type III	Col III	0.9951	C 1.04	0.93

C3_roHP		collagen	Synthesis		D 1.24	
C3M_HP	ns	MMP-9 generated fragments of type III collagen	Col III Degradation	0.1615	C 16.96 D 13.61	0.86
CTX-III_HP	ns	MMP-generated fragment of crosslinked type III collagen	Col III Degradation	0.4887	C 40.88 D 53.26	0.91
PRO-C4_HP	ns	Internal epitope in the 7S domain of type IV collagen	Col IV Synthesis	0.0739	C 195.98 D 183.12	0.84
C4M_HP	ns	MMP-generated fragment of the a1 chain of type IV collagen	Col IV Degradation	0.1014	C 8.89 D 7.42	0.84
PRO-C5_HP	Down*	C-terminal propeptide of type V collagen	Col V Synthesis	0.0458	C 33.17 D 35.88	0.82
PRO-C6_roHP	ns	C-terminal propeptide of type VI collagen alpha-3 chain	Col VI Synthesis	0.7222	C 0.27 D 0.27	0.92
C6M_HP	ns	MMP2-generated fragment of type VI collagen	Col VI Degradation	0.1097	C 22.31 D 23.41	0.83
PRO_C7 HP	Down*	BMP-I mediated neo-epitope in the NC-2 propeptide of type Vll collagen	Col VII Synthesis	0.0480	C 2.49 D 1.08	0.72
C7M	ND	Neo-epitope of MMP13 degradation of type Vll collagen	Col VII Degradation	NA	NA	NA
PRO-C9	ns	C-terminus of NC-I domain of the a1 chain of type IX collagen	Col IX Synthesis	0.9658	C 0.80 D 0.65	0.92

Table 1. Synthesis and degradation markers of Collagen I, II, III, IV, V, VII, and IX. Compared to controls, there were significant reductions in markers of Collagen I degradation, Collagen V synthesis, and Collagen VII synthesis. D/C: ratio of Dupuytren to control values. FC: fold change. **: <0.005, *: <0.05. ns: not significant. ND: undetectable in both disease and control cohorts.

We calculated collagen synthesis-to-degradation ratios for collagen types I, II, III, IV, and V. The Collagen I synthesis-to-degradation ratio, Pro-C1/C1M, was significantly greater in the DD cohort than in the control group (Fig 1D, $p = 0.024$). The remaining ratios were not significant (Col II, III, IV, VI) or could not be calculated because the degradation marker was either unavailable (Col V, IX) or not detectable in both disease and control cohorts (Col VII).

Differentially expressed blood proteins in DD

We used two orthogonal, unbiased proteomic methods: the aptamer-based SomaScan (SomaLogic; Boulder, CO) and liquid chromatography-tandem mass spectrometry (LC-MS/MS) (MacCoss Lab, University of Washington, WA, USA).

We used sixty-nine samples for SomaScan testing after quality control (36 DD and 33 controls). These represent 42 subjects, 27 of whom had second samples collected 6 to 14 months after the first (S1 Fig). The SomaScan panel measures 6995 protein binding sites applying to 5444 proteins.

Hypothesis-free approach

The 6995 aptamer measurements identified 54 proteins with statistically significant differences between the DD and control groups, with 24 overexpressed and 30 underexpressed after multiple-comparison adjustment (S1 Table). Fig 2 is a heatmap of these 54 protein expressions.

Fig 2. Heatmap of the 54 significant proteins in the hypothesis-free analysis. This heatmap shows natural log-transformed and standardized relative fluorescence units (RFU) for proteins (rows) across samples (columns). Red colors represent higher-than-average RFU values, and blue represents lower-than-average RFU values. Rows and/or columns are organized using hierarchical clustering, and cohorts are indicated by the top bar [purple: Dupuytren; green:

Control]. We performed pathway analysis of these 54 proteins to identify network relationships using STRING [28]. We found significant protein-protein interactions (PPI) in 29, with multiple enriched categories (Fig 3A, p-value = 4.55E-04). S2 Table summarizes categories of enriched gene groups, and Fig S2 provides a visual cross-reference of functional categories and individual genes. The dominant categories were coagulation and complement cascades, the extracellular matrix, enzyme inhibition, cell membrane structures, phosphorylation, and signaling pathways.

Fig 3. Hypothesis-Free DPRS and Protein-Protein Interactions. A) Network expression of 54 differentially expressed proteins. Of the 54 proteins, 30 had strong pathway connections in the network: ACAN, AKR1A1, C5, C6, CALCB, CASP3, CGA, CGB3, CPB1, CRKL, DSG2, EIF4H, FKBP5, G3BP2, GP1BB, GUSB, HGS, HSP90AA1, KNG1, MAP3K11, MBNL1, MBNL2, NRG4, OSCAR, PCSK9, POSTN, PRSS1, SERPINC1, SOCS3, SYK, TF, USP8, and YWHAB. B) The Hypothesis-free Diagnostic Proteomic Risk Score has an AUC-ROC value of 0.8. C) Hypothesis-free Diagnostic Proteomic Risk Scores (HF-DPRS) of the control vs Dupuytren cohorts. p-value = 5.28E-06.

Using SomaScan results, we aimed to develop a hypothesis-free indicator of DD diagnosis, the Diagnostic Proteomic Risk Score (DPRS), to estimate an individual's disease risk based on plasma protein abundance.

Hypothesis-free DPRS

We developed a hypothesis-free DPRS estimation based on two of the 54 proteins. These proteins, OSCAR (overexpressed) and SPART (underexpressed), had a low relative correlation (Pearson's correlation coefficient = -0.19) (Table 2), suggesting minimal interaction. Using this hypothesis-free DPRS as a diagnostic measure for DD achieved 79% accuracy in the training set (AUC 0.8) and 76.5% in the test set (Fig 3B), indicating predictive value for discriminating

between disease and control. Fig 3C shows a box plot of control and DD DPRS. The DPRS for controls and DD differed significantly by the Wilcoxon test (p-value = 2.5E-06).

Table 2. Hypothesis-free Diagnostic Proteomic Risk Score.

Protein	Eff	SE	p-value	FDR
Spartin	-11.62125	2.97479	0.000094	0.18
Oscar	13.99037	3.596067	0.0001	0.18

Table 2. Proteins of the Hypothesis-free DPRS. Eff = log (odds ratio comparing Dup to control) for a change of 1 in the log (protein data). SE: Standard error. FDR: False Discovery Rate (Adjusted p-value).

Hypothesis-based approach

We also used a hypothesis-based approach, identifying 328 relevant proteins from a literature search and available on the SomaScan platform (S3 Table). Twenty-three proteins in this subset showed statistically significant differences between DD and control, with nine overexpressed and 14 underexpressed after multiple-comparison adjustment (S4 Table).

We constructed PPI networks and performed enrichment analysis of these 23 proteins using STRING. We found significantly enriched PPI in 21 proteins with multiple enriched categories (Fig 4A, p-value = 1.35E-07). We found more enrichment categories and greater significance in the hypothesis-based than the hypothesis-free analysis, which may reflect a higher-yield group, selection bias, or both. S5 Table lists enriched gene categories, and Fig S3 provides a visual cross-reference between functional categories and individual genes.

Fig 4. Hypothesis-based DPRS and Protein-protein interactions. A) Network expression of 23 differentially expressed proteins. Of the 23 proteins, 20 had strong pathway connections: DAB2, SMAD1, USP8, PLAT, SFRP4, ACAN, DDR2, HPX, KNG1, LCN2, SERPINH1, TF, MAP2K1, PRKCA, STAT1, YWHAZ, POSTN, COL1A1, CASP3, and STAT3. B) The Hypothesis-based Diagnostic Proteomic Risk Score has an AUC-ROC value of 0.9. AUC-ROC (Area Under the Curve - Receiver Operating Characteristics) is an index of predictive accuracy. C) Hypothesis-free Diagnostic Proteomic Risk Scores (HF-DPRS) of the control vs Dupuytren cohorts. (p-value = 7.79E-09).

Hypothesis-based DPRS

We developed a hypothesis-based DPRS using 11 of 23 DE proteins identified in the hypothesis-based analysis. Six genes were underexpressed (*SMAD1, SH3BP2, LCN2, USP8, CSNK1G2, SERPINH1*) and five overexpressed (*CSMD1, POSTN, ACAN, AOC3, DDR2*). Six proteins were present in hypothesis-based and hypothesis-free DPRS analyses (Table 3). Our hypothesis-based DPRS achieved a training accuracy of 78.85% (AUC 0.9) and a test accuracy of 70.59% in distinguishing Dupuytren from control cohorts (Fig 4B). Fig 4C shows that DPRS distributions of Control and DD groups differ significantly (Wilcoxon test, p-value = 2.2E-09).

Table 3. Hypothesis-based Diagnostic Proteomic Risk Score.

Protein	Eff	SE	p-value	FDR
SMAD1*	-6.3649	1.877804	0.0007	0.12
CSMD1	5.397535	1.907423	0.00466	0.18
SH3BP2	-4.59151	1.582341	0.00371	0.18
POSTN*	4.305245	1.502627	0.00417	0.18
ACAN*	5.589134	1.75746	0.00147	0.12

LCN2	-4.73895	1.734879	0.0063	0.19
AOC3*	7.050175	2.62144	0.00716	0.2
DDR2	1.63418	0.595212	0.00604	0.19
USP8*	-3.30095	1.041269	0.00152	0.12
CSNK1G2*	-10.3331	3.593633	0.00404	0.18
SERPINH1	-2.6813	0.799538	0.0008	0.12

Table 3. Proteins of the Hypothesis-based DPRS. Eff = log (odds ratio comparing Dup to control) for a change of 1 in the log (protein data). SE: Standard error. FDR: False Discovery Rate (Adjusted p-value). * Six also had significant differential expression in the 54 proteins identified in the hypothesis-free analysis.

Evaluation of DRPS for prognosis

We explored the potential of each DPRS to profile DD prognosis. We used age at the time of the first DC procedure as an index of biological severity. We segregated our DD samples into subjects younger (11 specimens) or older (16 specimens) than age 50 at the time of their first DC procedure. We excluded from this analysis subjects younger than 50 at the time of their blood draw. A one-way ANOVA revealed a statistically significant difference in the means of the hypothesis-based DPRS across groups with different rates of pretreatment contracture progression (Fig S4; p-value = 0.0018). Conversely, we found no associations in the DPRS generated through the hypothesis-free approach.

Mass Spectrometry

The LC-MS dataset contained 48 samples: 27 DD and 21 controls. This assay identified 561 peptides. No peptides had statistically significant differences in abundance across groups (FDR > 0.25).

Mass-Spectrometry-SomaScan concordance

To further validate our SomaScan findings, we evaluated the MS results for concordance. Of the 54 significant proteins identified in the SomaScan analysis, six were also detected in the Mass Spectrometry findings: AOC3, POSTN, SERPINC1, TF, PCSK9, and KNG1. We ran the same analyses on these six proteins using Mass Spectrometry data. AOC3, POSTN, and SERPINC1 had adjusted p-values (FDR) <0.25 in both Mass Spec and SomaScan analyses (Table 4).

Table 4. Mass Spectrometry (MS) – SomaScan (SS) concordance.

Protein	Est MS	p-val MS	FDR MS	Est SS	p-val SS	FDR SS
AOC3	0.214854	0.076413	0.232677	0.116624	0.000845	0.217972
POSTN	0.410212	0.098842	0.232677	0.182892	0.000312	0.211479
SERPINC1	0.071331	0.116338	0.232677	0.091474	0.001500	0.225251
TF	0.035200	0.567393	0.829196	0.076715	0.000025	0.172072
PCSK9	0.165811	0.755318	0.829196	0.185675	0.001371	0.222267
KNG1	0.010065	0.829196	0.829196	0.065561	0.000490	0.217972

Table 4. Proteins identified in both MS and SS analyses. Six proteins identified by MS were also in the 54 proteins found in the hypothesis-free SS analysis: AOC3, POSTN, SERPINC1, TF, PCSK9, and KNG1. Of these, AOC3, POSTN, and SERPINC1 had False Discovery Rate (FDR, Adjusted p-value) <0.25 in both Mass Spec and SomaScan analyses. Est MS: Natural log fold change in protein abundance between Dupuytren disease cases and controls, measured by

Mass Spectrometry, estimated using a generalized estimating equation (GEE) model adjusted for age and gender. p-val MS: P-value for the Est MS, calculated from the robust standard error of the GEE model. FDR MS: False discovery rate (FDR)–adjusted p-value for Mass Spectrometry results, computed using the Benjamini–Hochberg procedure. Est SS: Natural log fold change in protein abundance between Dupuytren disease cases and controls, measured by SomaScan, estimated using a generalized estimating equation (GEE) model adjusted for age and gender. p-val SS: P-value for the Est SS, calculated from the robust standard error of the GEE model. FDR SS: False discovery rate (FDR)–adjusted p-value for SomaScan results, computed using the Benjamini–Hochberg procedure.

Discussion

This study aimed to identify candidate biomarkers that correlate with DD diagnosis as a first step toward a diagnostic DD blood test.

Dynamic biomarker panels are essential for developing preventive therapeutics for chronic diseases such as DD. The relevance of this study is that DD lacks such biomarkers. Blood is the most promising unexplored source of proteomic biomarkers for trend analysis.

There are no broad surveys of circulating proteins in DD. In addition, blood findings may not parallel tissue findings because of rapid degradation, intracellular or membrane-bound locations, post-translational variants, protein binding, and other mechanisms. Because of this, new and diverse discovery research is necessary to profile DD-associated blood protein biomarkers.

There are two common strategies for biomarker discovery: hypothesis-free and hypothesis-based. The hypothesis-free approach (also called unbiased or non-hypothesis-based) screens many markers and is the standard in systems biology and discovery research. The hypothesis-based strategy evaluates selected markers based on published information and is the most common model of DD research. We used both methods in this study.

Plasma collagen metabolites in DD

Collagen accumulation is the hallmark of DD. DD-affected tissues have unique proportions of collagen types I [29], III [30], IV [16], and V [29]. The most prominent tissue changes in the progression from preclinical to end-stage disease are increases in total Collagen I and the proportion of Collagen III [29].

Our hypothesis-based approach compared markers of collagen synthesis and degradation between the DD and control groups. Collagen turnover releases circulating peptides unique to the synthesis and degradation of each collagen type. In the absence of disease, synthesis and degradation markers are tightly coupled. Plasma synthesis-to-degradation marker ratios can indicate net collagen gain, loss, or homeostasis [18]. We used ELISA to measure plasma levels of 16 collagen metabolism markers across 8 collagen types. We summarize our findings in Table 1.

The DD cohort had normal Pro-C1 levels, a marker of Collagen I synthesis, but showed a statistically significant decrease in C1M, a marker of Collagen I degradation (Fig 1A), resulting in an elevated synthesis-to-degradation marker ratio in DD compared to controls (Fig 1D). These findings suggest DD collagen accumulation follows impaired Collagen I degradation rather than excess collagen synthesis. Both degradation-resistant collagen variants and reduced collagenase activity may contribute to reduced collagen degradation.

Dupuytren collagen has two features that increase resistance to enzymatic degradation. Typical Collagen I fibrils are heterotrimers of two Collagen I α1 strands and one Collagen I α2 strand. DD-affected tissues have an increased proportion of α1(I) homotrimeric Collagen I [31]. DD collagen also has more crosslinks stabilized by hydroxylation and glycosylation [32]. Both homotrimer Collagen I [33] and glycosylation-stabilized crosslinks [34] increase resistance to enzymatic cleavage.

DD-related dysregulation of collagenases and their inhibitors impairs collagen degradation by several mechanisms. TIMP1 (Tissue Inhibitor of Metalloproteinase 1) inhibits multiple MMPs and is elevated in the circulation of DD patients [35]. MMP1, MMP8, MMP13, and MMP14 gene polymorphisms are associated with Dupuytren disease [36, 37], including MMP14 partial loss-of-function variants [37]. MMP14 is necessary for MMP2 activation, and both enzymes facilitate myofibroblast contraction [38].

Two clinical findings support a relationship between impaired collagen degradation and DD. The first is the rapid onset of DD during treatment with a metalloproteinase inhibitor [39]. The second is abnormally slow matrix remodeling in DD. Enzymatic cleavage of collagen fibrils is necessary for matrix shortening [40], and impaired cleavage would slow this process. Slow matrix remodeling could explain why DD-related tissue shortening progresses more slowly than wound healing despite similar biology, and why DD surgery is associated with an increased risk of delayed wound healing [41]. The role of impaired collagen degradation in pathogenesis and intervention is unclear, and simply normalizing collagen degradation might have the undesirable effect of accelerating tissue contraction.

The hallmark of fibrotic diseases is the accumulation of collagen. Increased collagen synthesis contributes to collagen accumulation in pulmonary fibrosis [42], liver fibrosis [43], primary biliary cirrhosis [44], renal fibrosis [45], and cardiovascular disease [46]. Our finding of normal levels of

circulating Collagen I synthesis biomarkers in DD suggests that the mechanism of collagen accumulation in DD is not due to the increased collagen synthesis associated with these diseases. Although often used interchangeably with increased collagen synthesis, neither collagen accumulation nor upregulated collagen gene expression is, in itself, evidence of increased collagen synthesis. Cell culture studies show increased *COL1A1* and *COL1A2* mRNA expression in DD-derived fibroblasts [47, 48], but these RNA findings are not associated with increased collagen I protein production [48]. Our findings of normal Collagen I synthesis and impaired degradation inform future drug development research beyond the traditional focus of reducing collagen synthesis [49] to normalizing collagen degradation.

Collagen II markers were normal. We evaluated Collagen II markers because of the correlation between DD and psoriasis [50] and the finding of abnormal Collagen II in psoriasis [51]. We found no significant differences between groups in the Collagen II synthesis marker PRO-C2_HP, the degradation marker C2M_HP, or their ratios. The CALC2 synthesis marker was undetectable in both cohorts, preventing the calculation of CALC2 synthesis-to-degradation ratios.

Collagen III synthesis markers were normal, consistent with a prior report of normal circulating Collagen III synthesis marker amino-terminal propeptide of type III procollagen (PIIINP) in DD subjects [52]. Given the accumulation of Collagen III in DD, we expected to find elevated Collagen III synthesis-to-degradation marker ratios. Instead, we found normal Collagen III synthesis-to-degradation ratios. This finding may reflect that other proteases also degrade Collagen III, and we did not measure all potential collagen degradation fragments. To investigate further, we assayed a different Col III degradation marker, CTX-III_HP, on the remaining aliquots. Only 17 (10 DD, 7 Controls) of the initial 27 (13 DD, 14 Controls) leftover aliquots had sufficient residual volumes for this assay. Although this small subgroup's CTX-III

violin plot appearance suggested reduced degradation in DD compared to controls (Fig S5), this difference was not statistically significant.

We found significantly lower Pro-C5 levels, a marker of Collagen V synthesis, in the DD cohort than in controls (Fig 1B). This finding is unexplained. An increased percentage of Collagen V is reported in DD tissues [29], suggesting a high Collagen V synthesis-to-degradation ratio. However, we could not calculate this ratio because a Collagen V degradation marker was unavailable.

The DD cohort also had significantly lower levels of the Collagen VII synthesis marker Pro-C7 than controls (Fig 1C). We could not calculate Collagen VII synthesis-to-degradation ratios because Collagen VII degradation markers were undetectable in both cohorts. Although there are no reports of Collagen VII in DD, its role in matrix mechanobiology and elevated tissue levels in systemic sclerosis [53] make it a potential marker for collagen metabolism abnormalities in DD.

We found no significant differences in the remaining collagen markers. We measured Collagen IV markers because Collagen IV is elevated in DD tissues [16]. We assayed Collagen VI markers and ratios because prior pathway analysis suggests a role for Collagen VI in DD and other fibrotic diseases [54]. We selected Collagen IX markers based on unpublished data suggesting a role in DD. None of these markers or ratios showed significant differences between disease and control cohorts.

Plasma proteins and interactions in DD

In addition to the Nordic collagen fragment analysis, we analyzed whole proteins using the SomaScan aptamer-based platform. The SomaScan panel measures 6995 protein-binding sites

associated with 5444 proteins. S6 Table lists genes and gene aliases of proteins mentioned in this manuscript.

Our SomaScan hypothesis-free analysis identified 54 distinct proteins with plasma levels that were significantly different from those of controls. Twenty-four proteins showed increased levels, and 30 showed lower DD levels than controls (S1 Table). Our findings are consistent with existing literature.

The body of DD research publications mentions only seven of these 54 differentially expressed proteins: Aggrecan (*ACAN*), Amine Oxidase Copper Containing 3 (*AOC3*), Caspase-3 (*CASP3*), Periostin (*POSTN*), SMAD Family Member 1 (*SMAD1*), Spartin (*SPART*), and Ubiquitin carboxyl-terminal hydrolase 8 (*USP8*). Our differential expression findings concur with reports of *ACAN [55]*, *AOC3 [13]*, and *POSTN [56]* overexpression in tissue and *SMAD1 [57]*, *SPART [58]*, and *USP8 [58]* underexpression in cell culture. CASP3 levels were low in our findings, but are upregulated in a transcriptomic profiling report [55]. This finding is unexplained. *ACAN* is also near the variant rs6496519, which is associated with DD [59]. S1 Table summarizes the relevance of these 54 proteins and their parent genes to DD.

We constructed PPI networks and enrichment analysis of these 54 plasma proteins, revealing significantly enriched protein-protein interactions in 32, with multiple enriched protein groups and categories (Fig S2, S2 Table). These categories align with known Dupuytren cellular biology. Abnormalities in the KEGG category has04610 (complement and coagulation cascades) were consistent with DD pathway meta-analysis findings [60]. Complement fragments induce adhesion molecules that act on endothelial cells, consistent with DD-related perivascular clusters of immune cells and small vessel occlusion [13]. Complement fragments also activate mast cells that release TNF, a known DD pathway component [61], and histamine, a driver of itching, which is common in early-stage DD [62]. Cell membrane and extracellular

matrix signaling receptor binding of growth factors, cytokines, and other signaling factors play pivotal roles in DD pathobiology [14]. Protein phosphorylation processes are consistent with increased phosphorylated STAT1, STAT3, SMAD2, SMAD3, and ERK1/2 in DD tissues [57, 63, 64]. The enriched Reactome HSA-162582 (Signal Transduction) pathway is noteworthy, as it includes signaling by TGF-Beta, WNT, and NOTCH, all of which are prominent in DD biology [65].

We based our hypothesis-free DPRS on high levels of Osteoclast-associated immunoglobulin-like receptor (*OSCAR*) and low levels of Spartin (*SPART*) (Table 2). Our finding of elevated OSCAR levels is interesting because Collagen I is an OSCAR ligand. OSCAR also stimulates T-cells to release TNF [66], a component of DD biology [61]. Our finding of decreased *SPART* levels is consistent with low *SPART* expression in DD fibroblasts [58]. SPART is also associated with Epidermal Growth Factor Receptor (EGFR) degradation and transport to the cell membrane [67], consistent with increased ratios of intracellular to cell membrane EGFR levels observed in DD [68].

In addition to the hypothesis-free analysis, we conducted a hypothesis-based analysis using a subset of SomaScan proteins selected from an independent literature review (S3 Table). We identified 23 proteins in this subset with significantly different plasma levels compared to controls. Nine proteins had higher levels in DD than in controls, and fourteen had lower levels. Nine proteins were present in both hypothesis-free and hypothesis-based groups. Our findings are consistent with existing literature. S4 Table summarizes the potential relationships among these proteins, their parent genes, and DD.

With our hypothesis-free analysis, we performed a STRING PPI analysis of the hypothesis-based findings to identify network relationships of the 23 proteins. We found significantly enriched protein-protein interactions in 21 with multiple enriched categories (p-value = 1.35E-

07, S5 Table). This analysis implicated additional enrichment categories beyond those from the hypothesis-free analysis. Myofibroblast differentiation, proliferation, motility, WNT signaling, and interleukin pathways are unsurprising, given their known roles in DD biology [10, 69]. Cancer pathway associations are also unsurprising, given the correlations between DC and carcinomas and sarcomas [70, 71]. Infection-related pathways were unexpected and were exclusively associated with viral and parasitic infection categories. This finding might be due to a hidden variable of tissue repair biology, which overlaps interleukin-driven parasitic immune defense biology and interleukin-related DD biology.

This hypothesis-based analysis generated data for a second Diagnostic Proteomic Risk Score (DPRS) calculated from 11 proteins (Table 3). Fig 4A shows the AUC-ROC of this panel (AUC = 0.9), and Fig 4B shows the DPRS based on this panel, distinguishing DD from control cohorts.

We evaluated the potential of each DPRS for staging. Recurrence after a procedure is the benchmark of Dupuytren's biological severity. Traditionally, surgeons use clinical factors such as early age of onset, affected family members, and disease locations other than the palms to predict post-procedure recurrence. However, the study's inclusion criteria included these factors, so we could not use them to subset our Dupuytren cohort. Instead, we used age at the time of the first DC procedure. Recurrence is more common in patients who are younger at their first DC procedure [72-76]. We evaluated each DPRS to distinguish Dupuytren subjects who had their first corrective procedure before age 50 from those who had their first correction at age 50 or older. The hypothesis-based DPRS distinguished DD subjects who underwent their first DC procedure before age 50 from those who underwent their first DC procedure after age 50 ($p=0.0018$), suggesting potential use as a staging and predictive tool. An unexpected and unexplained finding is that DPRS scores were higher in DD than in controls, but hypothesis-

based DPRS scores were higher in DD patients who had their first procedure after age 50 than in those who were younger at the time of their first corrective procedure.

Although Mass Spectrometry did not reveal statistically significant differences in abundance across cohorts, there was statistically significant concordance between Mass Spec and SomaScan findings. The Mass Spec data contained 6 of the 54 proteins with statistically significant differences between disease and control cohorts using the hypothesis-free SomaScan data analysis: Amine Oxidase Copper Containing 3 *AOC3*, Periostin *POSTN*, Serpin Family C Member 1 *SERPINC1*, Transferrin *TF*, Proprotein Convertase Subtilisin/Kexin Type 9 *PCSK9*, and Kininogen 1 *KNG1*. Table 4 compares the results of the SomaScan and Mass Spectrometry data analysis. A pathway analysis of these six proteins identified two highly significant Reactome categories (S7 Table). In addition to protein phosphorylation noted above, Reactome HSA-381426 involving Insulin-like Growth Factor *IGF* and Insulin-like Growth Factor Binding Proteins *IGFBP*s is relevant because of the role of IGF-II and IGFBP-6 in regulating Dupuytren fibroblast proliferation and contractility [77].

This study has limitations. Statistical disadvantages included the small sample sizes across all assays, and the large number of aptamers in the SomaScan assay. Although our findings align with current research on Dupuytren proteomics, there are differences. Elevated serum TIMP1 [35] and TNF [69] have been reported in DD, but we found no statistically significant DE between disease and control groups. This discrepancy may reflect that SomaScan assays target specific protein conformations, whereas ELISA measures all conformations.

Conclusions

We used ELISA, aptamer, and mass spectrometry assays to identify differential plasma proteomic signatures between DD and control cohorts. We found significant DD-related

proteomic abnormalities in both circulating collagen metabolism peptide fragments and whole proteins. This study is the first to provide evidence suggesting net collagen accumulation in DD results from normal collagen synthesis and impaired collagen degradation, challenging the model of excess collagen synthesis and distinguishing DD from other organ fibroses. We independently analyzed proteins from the same cohorts. Our hypothesis-free analysis of 5444 proteins revealed 54 with statistically significant differences between the DD and control cohorts. Our independent hypothesis-based analysis of 328 proteins selected from the literature review identified 23 with statistically significant differences. We developed two Dupuytren Diagnostic Proteomic Risk Scores, one based on hypothesis-free and the other based on hypothesis-driven analyses. We used pathway analyses to identify enrichments in the DD protein-protein network, confirming known DD interactions and revealing previously unreported DD pathway categories. Finally, we showed our hypothesis-based DPRS correlated with the subject's age at the time of the first DD procedure, an index of biological severity. These findings suggest that a validated, hypothesis-based DPRS could guide management and the development of DD therapeutics.

We recommend a larger study to validate our findings on the metabolites of Collagen I, III, V, and VII. We also recommend a validating study of 68 unique proteins identified in the protein aptamer analysis (54 in the hypothesis-free analysis and 23 in the hypothesis-based analysis, with 9 in both groups). Testing only the subset of the 68 most pertinent proteins would increase statistical power. Individual ELISA assays would be cost-prohibitive. An alternative approach would be to develop a custom multiplex panel for the 13 proteins in our two DPRS [14] to validate our DPRS and to assess the correlation with our hypothesis-based DPRS on age at the first DD procedure. Our findings strongly support the need to fund and conduct more extensive validating studies of circulating collagen metabolites and proteins in DD. This biomarker

research is fundamental to developing DD diagnostic tests, staging DD, and informing the development of therapeutic drugs for DD.

Acknowledgments

Gail Solomon assisted with manuscript writing.

Databank and study support from FORWARD, the National Databank for Rheumatic Diseases, is gratefully acknowledged.

Author Contributions

BH: Formal Analysis, Data Curation, Methodology, Software, Validation, Visualization, Writing original draft, review, and editing. PS: Formal Analysis, Data Curation, Methodology, Software, Validation, Visualization, Writing original draft, review, and editing. AL: Formal Analysis, Software, Validation, Visualization. AG: Formal Analysis, Software, Validation, Visualization. CB: Formal Analysis. MK: Formal Analysis, Methodology. SN: Formal Analysis. CE: Conceptualization, Data Curation, Investigation, Methodology, Visualization, Writing original draft, review, and editing.

Supporting information

S1 Fig. Distribution of samples to laboratories. Forty-five subjects provided initial samples. Seventeen of these subjects had second samples drawn at least 6 months after the first. Mass spec lab 1 performed analysis on the initial 45 samples. Mass spec lab 2 and collagen metabolite analyses were performed on redraw specimens. Aptamer-based analysis was performed on both initial and redraw specimens. Three of the original forty-five samples for Aptamer analysis failed quality control, leaving 23 DD and 19 Controls available for analysis.

S2 Fig. Protein-protein network enrichment categories in the hypothesis-free analysis. Thirty-two differentially expressed proteins showed significant network enrichment (p.adj < 0.05) in the following biological categories. C&C: coagulation and complement cascades, ECM: extracellular matrix, ENZ: Enzyme inhibition, MBR: cell membrane structures, PPL: phosphorylation, SGN: other signaling pathways.

S3 Fig. Protein-protein network enrichment categories in the hypothesis-based analysis. Twenty-one differentially expressed proteins showed significant network enrichment (p.adj < 0.05) in the following biological categories. CAN: Cancer, C&C: coagulation and complement cascades, ECM: extracellular matrix, INL: interleukin interactions, INF: infection, MBR: cell membrane structures, MFB: myofibroblast differentiation, proliferation, and motility, PPL: phosphorylation, SGN: other signaling pathways, WNT: WNT pathways. Hypothesis-based selection bias from a preselected list of candidate proteins may influence the enrichment results.

S4 Fig. Hypothesis-based DPRS correlates with age at the time of the first Dupuytren procedure. This 11-protein Hypothesis-Based Dupuytren Proteomic Risk Score (HB-DPRS) distinguished DD subjects with different disease progression rates based on whether the subject was younger than 50 vs. 50 or older during their first corrective procedure (p=0.0018).

S5 Fig. Differential expression of Dupuytren vs. control Collagen III degradation marker CTX-III. Although these violin plots visually suggest reduced Collagen III degradation marker CTX-III values in DD compared to controls, this difference was not significant (p-value = 0.4887). These data were from 17 of the 27 samples used for the other collagen metabolism markers, due to insufficient volumes in 10 samples. Because small cohorts magnify the effects of outliers, we recommend repeating these assays on larger cohorts.

S1 Table. 54 Differentially expressed genes in the SomaScan Hypothesis-free analysis. Of the 6995 aptamers in the Hypothesis-free analysis, 54 proteins showed statistically significant

differences between the DD and control groups, with 24 overexpressed and 30 underexpressed after adjusting for multiple comparisons. Nine of these proteins were identified in both hypothesis-free and hypothesis-based analyses, as indicated by *. Plain italics indicate an indirect DD relationship, if any, to the protein; bold italics indicate a direct relationship between published DD findings and the protein [10, 13, 55, 57, 58, 61, 66, 68, 71, 78, 82, 84-126]. In the Notes column, "Referred to" means the referenced publication referred to the gene by an alias name. Exp: DD expression compared to controls. p-val: p-value of expression difference. FDR: False discovery rate (adjusted p-value. Nodes: number of pathway analysis connections (nodes) of this protein to others in this group with a medium confidence interaction score (0.400) and an FDR<=0.05. Notes: potential relationship to DD biology. DOI: DOIs of publications referenced in Notes. Cat: categories of possible relationships to DD: 1. Apoptosis and senescence (3 genes); 2. Bioinformatics (9 genes); 3. Clinical and demographic (6 genes); 4. Extracellular matrix (6 genes); 5. Fibroblast and myofibroblast cytoskeleton, membrane, and motility (10 genes); 6. Fibroblast and myofibroblast differentiation and transcriptome (7 genes); 7. Vascular and perivascular (9 genes); Unclear relationship (16 genes).

S2 Table. Functionally enriched pathways derived from the 54 differentially expressed proteins in the hypothesis-free analysis. ID: Enriched category name. STR: Strength of protein-protein interaction (PPI). FDR: False Discovery Rate (Adjusted p-value). Overall PPI enrichment p-value: 0.000455. Figure 4 summarizes enriched pathways for individual genes.

S3 Table. 328 protein-coding genes in the SomaLogic hypothesis-based analysis. We combined three literature-based search strategies to identify candidate Dupuytren-related genes for hypothesis-based analytics. We first collected 2547 full-text publications from 1980 to 2023 that included at least three instances of the search terms "Dupuytren*" and/or "palmar fibroma*". In the first strategy, we searched each publication for 4527 potential Dupuytren-related genes

and their 33907 gene name aliases. This search identified 326 unique proteins or parent genes mentioned at least three times in at least one publication. The second method identified 117 selected collagen metabolism-related proteins or their parent genes that appeared at least once in at least one of these publications. The third method identified potentially DD-related single-nucleotide polymorphisms (SNPs) reported in these publications and compiled a list of 369 genes adjacent to these SNPs. We merged these three lists, resulting in 546 unique protein-coding genes, 328 of which matched proteins on the SomaScan panel, which contains 6995 protein-binding sites. Proteins expressed by these 328 genes were the targets of our hypothesis-based analysis.

S4 Table. 23 Differentially expressed genes in the Hypothesis-based analysis. Of the 328 aptamers in the Hypothesis-based analysis, 23 had statistically significant differences between DD and control, with nine overexpressed and fourteen underexpressed after adjusting for multiple comparisons. Nine of these genes appeared in hypothesis-free and hypothesis-based analyses, as indicated by *. Plain italics indicate an indirect DD relationship, if any, to the protein; bold italics indicate a direct relationship between published DD findings and the protein [10, 13, 31, 33, 37, 55, 57, 58, 59, 64, 78, 79, 84, 87, 88, 92, 93, 94, 108, 109, 117-119, 125-143]. In the Notes column, "Referred to" means the referenced publication referred to the gene by an alias name. Exp: DD expression compared to controls. FDR: False Discovery Rate (Adjusted p-value) of expression difference. Nodes: number of pathway analysis connections (nodes) of this protein to others in this group with a medium confidence interaction score (0.400) and an FDR<=0.05. Notes: potential relationship to DD biology. DOI: DOIs of publications referenced in Notes. Cat: categories of possible relationships to DD: 1. Apoptosis and senescence (2 genes); 2. Bioinformatics (7 genes); 3. Clinical and demographic (3 genes); 4. Extracellular matrix (9 genes); 5. Fibroblast and myofibroblast cytoskeleton, membrane, and

motility (6 genes); 6. Fibroblast and myofibroblast differentiation and transcriptome (5 genes); 7. Vascular and perivascular (4 genes).

S5 Table. Functionally enriched pathways derived from the 23 differentially expressed proteins in the hypothesis-based analysis. ID: Enriched category name. STR: Strength of protein-protein interaction (PPI). FDR: False Discovery Rate (Adjusted p-value). Overall PPI enrichment p-value: 1.35E-07. Hypothesis-based candidate protein preselection may influence enrichment results. Figure 6 summarizes enriched pathways for individual genes.

S6 Table. Genes referenced in the manuscript and their aliases. This table lists all gene names referenced in the manuscript, their UniProt identifiers, protein names, and gene aliases.

S7 Table. Enriched pathways in Mass Spec - SomaScan concordant genes. Six proteins identified by Mass Spectrometry had statistically significant differences between Dupuytren and control cohorts in the SomaScan analysis, representing genes AOC3, POSTN, SERPINC1, TF, PCSK9, and KNG1. Within this network, AOC3, POSTN, and PCSK9 had strong pathway connections, and PCSK9, SERPINC1, TF, and KNG1 had functionally enriched pathways. PPI enrichment p-value: 0.00987. STR: Strength of association. FDR: False Discovery Rate (adjusted p-value).

Data availability

All the data and analytic scripts necessary to replicate the findings are available in the GitHub repository Dup_Blood_Proteomic_Data at https://github.com/Dupuytren/Dup_Blood_Proteomic_Data.

Competing interest statement

The authors declare the following competing interests: Morten Karsdal, Cecilie Bager, and Signe Holm Nielsen are employees of Nordic Bioscience and hold stocks in Nordic Bioscience. No other competing interests have been declared. This does not alter the authors' adherence to PLOS ONE policies on sharing data and materials.

References

1. Macaulay D, Ivanova J, Birnbaum H, Sorg R, Skodny P. Direct and indirect costs associated with Dupuytren's contracture. J Med Econ. 2012;15(4):664–71. Epub 2012/03/01. doi: 10.3111/13696998.2012.670678. PubMed PMID: 22369346.

2. Broekstra DC, Kuo RYL, Burn E, Prieto-Alhambra D, Furniss D. Dupuytren Disease: Prevalence, Incidence, and Lifetime Risk of Surgical Intervention. A Population-Based Cohort Analysis. Plast Reconstr Surg. 2023;151(3):581–91. Epub 20221122. doi: 10.1097/PRS.0000000000009919. PubMed PMID: 36730480; PubMed Central PMCID: PMCPMC9944385.

3. Mendelaar NHA, Poelstra R, van Nieuwenhoven CA, Slijper HP, Feitz R, Hovius SER, et al. Outcome of Recurrent Surgery in Dupuytren's Disease: Comparison with Initial Treatment. Plast Reconstr Surg. 2019;144(5):828e–35e. Epub 2019/08/10. doi: 10.1097/PRS.0000000000006150. PubMed PMID: 31397794.

4. Goodman AD, Gil JA, Starr AM, Akelman E, Weiss A-PC. Incidence of Serious Complications in Hand Surgery: A 10-Year Review. The Journal of Hand Surgery. 2016;41(9):S27–S8. doi: 10.1016/j.jhsa.2016.07.047.

5. Schindelar L, McEntee R, D'Amore T, Beredjiklian P, Lutsky K. Unplanned Return to the Operating Room in Upper-Extremity Surgery: Incidence and Reason for Return. J Hand Surg Am. 2021;46(8):715 e1– e12. Epub 20210514. doi: 10.1016/j.jhsa.2021.01.019. PubMed PMID: 33994259.

6. Denkler K. Surgical complications associated with fasciectomy for dupuytren's disease: a 20-year review of the English literature. Eplasty. 2010;Jan 27(10):e15. PubMed Central PMCID: PMCPMC2828055.

7. Alser O, Craig RS, Lane JCE, Prats-Uribe A, Robinson DE, Rees JL, et al. Serious complications and risk of re-operation after Dupuytren's disease surgery: a population-based cohort study of 121,488 patients in England. Sci Rep. 2020;10(1):16520. Epub 2020/10/07. doi: 10.1038/s41598-020-73595-y. PubMed PMID: 33020582; PubMed Central PMCID: PMCPMC7536429.

8. Degreef I, De Smet L. Dupuytren's disease: a predominant reason for elective finger amputation in adults. Acta Chir Belg. 2009;109(4):494–7. Epub 2009/10/07. doi: 10.1080/00015458.2009.11680467. PubMed PMID: 19803262.

9. Larsen S, Krogsgaard DG, Aagaard Larsen L, Iachina M, Skytthe A, Frederiksen H. Genetic and environmental influences in Dupuytren's disease: a study of 30,330 Danish twin pairs. J Hand Surg Eur Vol. 2015;40(2):171–6. Epub 2014/05/20. doi: 10.1177/1753193414535720. PubMed PMID: 24835475; PubMed Central PMCID: PMCPMC4810018.

10. Dolmans GH, Werker PM, Hennies HC, Furniss D, Festen EA, Franke L, et al. Wnt signaling and Dupuytren's disease. N Engl J Med. 2011;365(4):307–17. Epub 2011/07/08. doi: 10.1056/NEJMoa1101029. PubMed PMID: 21732829.

11. Riesmeijer SA, Manley OWG, Ng M, Nolte IM, Broekstra DC, Werker PMN, et al. A Weighted Genetic Risk Score Predicts Surgical Recurrence Independent of High-Risk Clinical Features in Dupuytren's Disease. Plast Reconstr Surg. 2019;143(2):512–8. Epub 2019/01/29. doi: 10.1097/PRS.0000000000005208. PubMed PMID: 30688894; PubMed Central PMCID: PMCPMC6358194.

12. Iqbal SA, Hindocha S, Farhatullah S, Paus R, Bayat A. Dupuytren’s Disease Shows Populations of Hematopoietic and Mesenchymal Stem-Like Cells Involving Perinodular Fat and

Skin in Addition to Diseased Fascia: Implications for Pathogenesis and Therapy. Dupuytren's Disease and Related Hyperproliferative Disorders2012. p. 167–74.

13. Mayerl C, Del Frari B, Parson W, Boeck G, Piza-Katzer H, Wick G, et al. Characterisation of the inflammatory response in Dupuytren's disease. J Plast Surg Hand Surg. 2016;50(3):171–9. Epub 2016/02/09. doi: 10.3109/2000656X.2016.1140054. PubMed PMID: 26852784.

14. Gonga-Cave BC, Pena Diaz AM, O'Gorman DB. Biomimetic analyses of interactions between macrophages and palmar fascia myofibroblasts derived from Dupuytren's disease reveal distinct inflammatory cytokine responses. Wound Repair Regen. 2021;29(4):627–36. Epub 20210611. doi: 10.1111/wrr.12928. PubMed PMID: 34212454.

15. Halliday NL, Rayan GM, Zardi L, Tomasek JJ. Distribution of ED-A and ED-B containing fibronectin isoforms in Dupuytren's disease. J Hand Surg Am. 1994;19(3):428–34. Epub 1994/05/01. doi: 10.1016/0363-5023(94)90057-4. PubMed PMID: 8056970.

16. Magro G, Fraggetta F, Travali S, Lanzafame S. Immunohistochemical expression and distribution of alpha2beta1, alpha6beta1, alpha5beta1 integrins and their extracellular ligands, type IV collagen, laminin and fibronectin in palmar fibromatosis. Gen Diagn Pathol. 1997;143(4):203–8. Epub 1998/03/07. PubMed PMID: 9489951.

17. Broekstra DC, Lanting R, Werker PMN, van den Heuvel ER. Disease Course of Primary Dupuytren Disease: 5-Year Results of a Prospective Cohort Study. Plast Reconstr Surg. 2022;149(6):1371–8. Epub 20220411. doi: 10.1097/PRS.0000000000009115. PubMed PMID: 35404338.

18. Karsdal MA, Leeming DJ, Henriksen K, Bay-Jensen AC, Nielsen SH, CL B. Biochemistry of Collagens, Laminins and Elastin. Boston: Elsevier; 2019.

19. Hughes CS, Moggridge S, Muller T, Sorensen PH, Morin GB, Krijgsveld J. Single-pot, solid-phase-enhanced sample preparation for proteomics experiments. Nat Protoc. 2019;14(1):68–85. Epub 2018/11/23. doi: 10.1038/s41596-018-0082-x. PubMed PMID: 30464214.

20. Leutert M, Rodriguez-Mias RA, Fukuda NK, Villen J. R2-P2 rapid-robotic phosphoproteomics enables multidimensional cell signaling studies. Mol Syst Biol. 2019;15(12):e9021. doi: 10.15252/msb.20199021. PubMed PMID: 31885202; PubMed Central PMCID: PMCPMC6920700.

21. Amodei D, Egertson J, MacLean BX, Johnson R, Merrihew GE, Keller A, et al. Improving Precursor Selectivity in Data-Independent Acquisition Using Overlapping Windows. J Am Soc Mass Spectrom. 2019;30(4):669–84. Epub 20190122. doi: 10.1007/s13361-018-2122-8. PubMed PMID: 30671891; PubMed Central PMCID: PMCPMC6445824.

22. Searle BC, Pino LK, Egertson JD, Ting YS, Lawrence RT, MacLean BX, et al. Chromatogram libraries improve peptide detection and quantification by data independent acquisition mass spectrometry. Nat Commun. 2018;9(1):5128. Epub 2018/12/05. doi: 10.1038/s41467-018-07454-w. PubMed PMID: 30510204; PubMed Central PMCID: PMCPMC6277451.

23. Hoofnagle AN, Becker JO, Oda MN, Cavigiolio G, Mayer P, Vaisar T. Multiple-reaction monitoring-mass spectrometric assays can accurately measure the relative protein abundance in complex mixtures. Clin Chem. 2012;58(4):777–81. Epub 20120203. doi: 10.1373/clinchem.2011.173856. PubMed PMID: 22307200; PubMed Central PMCID: PMCPMC3665768.

24. Gold L, Ayers D, Bertino J, Bock C, Bock A, Brody EN, et al. Aptamer-based multiplexed proteomic technology for biomarker discovery. PLoS One. 2010;5(12):e15004. Epub 20101207.

doi: 10.1371/journal.pone.0015004. PubMed PMID: 21165148; PubMed Central PMCID: PMCPMC3000457.

25. Berrone E, Chiorino G, Guana F, Benedetti V, Palmitessa C, Gallo M, et al. SOMAscan Proteomics Identifies Novel Plasma Proteins in Amyotrophic Lateral Sclerosis Patients. Int J Mol Sci. 2023;24(3). Epub 20230118. doi: 10.3390/ijms24031899. PubMed PMID: 36768220; PubMed Central PMCID: PMCPMC9916400.

26. Network TCRA. gee: Generalized Estimation Equation Solver 2023 [01/06/2023]. Available from: https://cran.r-project.org/package=gee.

27. Kuhn M. Building Predictive Models in R Using the caret Package. Journal of Statistical Software [Internet]. 2008; 28(5).

28. Szklarczyk D, Kirsch R, Koutrouli M, Nastou K, Mehryary F, Hachilif R, et al. The STRING database in 2023: protein-protein association networks and functional enrichment analyses for any sequenced genome of interest. Nucleic Acids Res. 2023;51(D1):D638–D46. doi: 10.1093/nar/gkac1000. PubMed PMID: 36370105; PubMed Central PMCID: PMCPMC9825434.

29. Bailey AJ. Collagen. In: McFarlane R, McGrouther D, Flint M, editors. Dupuytren's Disease Biology and Treatment. Hand and Upper Limb Series. 5. Edinburg: Churchill Livingstone; 1990.

30. Bailey AJ, Sims TJ, Gabbiani G, Bazin S, LeLous M. Collagen of Dupuytren's disease. Clin Sci Mol Med. 1977;53(5):499–502. Epub 1977/11/01. doi: 10.1042/cs0530499. PubMed PMID: 589933.

31. Williamson K, Cooper G, Lee KJ, Beamish EL, Simpson D, Carter A, et al. Active synthesis of type I collagen homotrimer in Dupuytren's fibrosis is unaffected by anti-TNF-α treatment. bioRxiv preprint 2023. doi: 10.1101/2020.07.13.195107.

32. Bazin S, Le Lous M, Duance VC, Sims TJ, Bailey AJ, Gabbiani G, et al. Biochemistry and histology of the connective tissue of Dupuytren's disease lesions. Eur J Clin Invest. 1980;10(1):9–16. Epub 1980/02/01. doi: 10.1111/j.1365-2362.1980.tb00003.x. PubMed PMID: 6768572.

33. Han S, Makareeva E, Kuznetsova NV, DeRidder AM, Sutter MB, Losert W, et al. Molecular mechanism of type I collagen homotrimer resistance to mammalian collagenases. J Biol Chem. 2010;285(29):22276–81. Epub 2010/05/14. doi: 10.1074/jbc.M110.102079. PubMed PMID: 20463013; PubMed Central PMCID: PMCPMC2903388.

34. Snedeker JG, Gautieri A. The role of collagen crosslinks in ageing and diabetes - the good, the bad, and the ugly. Muscles Ligaments Tendons J. 2014;4(3):303–8. Epub 2014/12/10. PubMed PMID: 25489547; PubMed Central PMCID: PMCPMC4241420.

35. Ulrich D, Hrynyschyn K, Pallua N. Matrix metalloproteinases and tissue inhibitors of metalloproteinases in sera and tissue of patients with Dupuytren's disease. Plast Reconstr Surg. 2003;112(5):1279–86. Epub 2003/09/25. doi: 10.1097/01.PRS.0000081462.40448.49. PubMed PMID: 14504511.

36. Rodrigues MP, Tissi LH, Oliveira VM, Wistuba G, Araujo FB, Mattar-Junior R, et al. MMP-1, MMP-8, and MMP-13 Gene Polymorphisms and Haplotype Is a Risk Factor for Dupuytren Contracture: A Case-Control Study. Hand (N Y). 2024:15589447241242818. Epub 20240425. doi: 10.1177/15589447241242818. PubMed PMID: 38660990.

37. Itoh Y, Ng M, Wiberg A, Inoue K, Hirata N, Paiva KBS, et al. A common SNP risk variant MT1-MMP causative for Dupuytren's disease has a specific defect in collagenolytic activity.

Matrix Biol. 2021;97:20–39. Epub 2021/02/17. doi: 10.1016/j.matbio.2021.02.003. PubMed PMID: 33592276.

38. Wilkinson JM, Davidson RK, Swingler TE, Jones ER, Corps AN, Johnston P, et al. MMP-14 and MMP-2 are key metalloproteases in Dupuytren's disease fibroblast-mediated contraction. Biochim Biophys Acta. 2012;1822(6):897–905. Epub 2012/02/22. doi: 10.1016/j.bbadis.2012.02.001. PubMed PMID: 22342364.

39. Krzeski P, Buckland-Wright C, Balint G, Cline GA, Stoner K, Lyon R, et al. Development of musculoskeletal toxicity without clear benefit after administration of PG-116800, a matrix metalloproteinase inhibitor, to patients with knee osteoarthritis: a randomized, 12-month, double-blind, placebo-controlled study. Arthritis Res Ther. 2007;9(5):R109. Epub 2007/10/26. doi: 10.1186/ar2315. PubMed PMID: 17958901; PubMed Central PMCID: PMCPMC2212568.

40. Castella LF, Buscemi L, Godbout C, Meister JJ, Hinz B. A new lock-step mechanism of matrix remodelling based on subcellular contractile events. J Cell Sci. 2010;123(Pt 10):1751–60. Epub 2010/04/30. doi: 10.1242/jcs.066795. PubMed PMID: 20427321.

41. Bismil Q, Bismil M, Bismil A, Neathey J, Gadd J, Roberts S, et al. The development of one-stop wide-awake dupuytren's fasciectomy service: a retrospective review. JRSM Short Rep. 2012;3(7):48. Epub 2012/08/22. doi: 10.1258/shorts.2012.012050. PubMed PMID: 22908029; PubMed Central PMCID: PMCPMC3422854.

42. Organ LA, Duggan AR, Oballa E, Taggart SC, Simpson JK, Kang'ombe AR, et al. Biomarkers of collagen synthesis predict progression in the PROFILE idiopathic pulmonary fibrosis cohort. Respir Res. 2019;20(1):148. Epub 20190712. doi: 10.1186/s12931-019-1118-7. PubMed PMID: 31299951; PubMed Central PMCID: PMCPMC6624898.

43. Liu T, Wang X, Karsdal MA, Leeming DJ, Genovese F. Molecular serum markers of liver fibrosis. Biomark Insights. 2012;7:105–17. Epub 20120723. doi: 10.4137/BMI.S10009. PubMed PMID: 22872786; PubMed Central PMCID: PMCPMC3412619.

44. Vesterhus M, Nielsen MJ, Hov JR, Saffioti F, Manon-Jensen T, Leeming DJ, et al. Comprehensive assessment of ECM turnover using serum biomarkers establishes PBC as a high-turnover autoimmune liver disease. JHEP Rep. 2021;3(1):100178. Epub 20200903. doi: 10.1016/j.jhepr.2020.100178. PubMed PMID: 33225252; PubMed Central PMCID: PMCPMC7666353.

45. Han DC, Isono M, Hoffman BB, Ziyadeh FN. High glucose stimulates proliferation and collagen type I synthesis in renal cortical fibroblasts: mediation by autocrine activation of TGF-beta. J Am Soc Nephrol. 1999;10(9):1891–9. doi: 10.1681/ASN.V1091891. PubMed PMID: 10477140.

46. Genovese F, Goncalves I, Holm Nielsen S, Karsdal MA, Edsfeldt A, Nilsson J, et al. Plasma levels of PRO-C3, a type III collagen synthesis marker, are associated with arterial stiffness and increased risk of cardiovascular death. Atherosclerosis. 2024;388:117420. Epub 20231210. doi: 10.1016/j.atherosclerosis.2023.117420. PubMed PMID: 38128431.

47. Satish L, Gallo PH, Baratz ME, Johnson S, Kathju S. Reversal of TGF-beta1 stimulation of alpha-smooth muscle actin and extracellular matrix components by cyclic AMP in Dupuytren's-derived fibroblasts. BMC Musculoskelet Disord. 2011;12:113. Epub 2011/05/27. doi: 10.1186/1471-2474-12-113. PubMed PMID: 21612641; PubMed Central PMCID: PMCPMC3125251.

48. van Beuge MM, Ten Dam EJ, Werker PM, Bank RA. Matrix and cell phenotype differences in Dupuytren's disease. Fibrogenesis Tissue Repair. 2016;9:9. Epub 2016/07/02.

929 doi: 10.1186/s13069-016-0046-0. PubMed PMID: 27366208; PubMed Central PMCID:
930 PMCPMC4928329.

931 49. Lambi AG, Popoff SN, Benhaim P, Barbe MF. Pharmacotherapies in Dupuytren Disease:
932 Current and Novel Strategies. J Hand Surg Am. 2023. Epub 20230317. doi:
933 10.1016/j.jhsa.2023.02.003. PubMed PMID: 36935324.

934 50. Patel M, Freeman NR, Dhaliwal S, Wright N, Daoud Y, Ryan C, et al. The prevalence of
935 Dupuytren contractures in patients with psoriasis. Clin Exp Dermatol. 2014;39(8):894–9. Epub
936 2014/09/10. doi: 10.1111/ced.12424. PubMed PMID: 25196833.

937 51. Holm Nielsen S, Magee C, Groen SS, Sinkeviciute D, Bay-Jensen AC, Karsdal MA, et al.
938 Differentiating patients with psoriasis from psoriatic arthritis using collagen biomarkers. Clin Exp
939 Rheumatol. 2022. Epub 20220728. doi: 10.55563/clinexprheumatol/jmt9jv. PubMed PMID:
940 35916294.

941 52. Gassier N, Brenner P, Berger A, Delbruck A. Biochemical Parameters for the Diagnosis
942 of Dupuytren's Disease. In: Berger A, Delbruck A, Brenner P, Hinzmann B, editors. Dupuytren's
943 Disease Pathobiochemistry and Clinical Management. Berlin: Springer-Verlag; 1994. p. 94–8.

944 53. Sand JMB, Lamy P, Juhl P, Siebuhr AS, Iversen LV, Nawrocki A, et al. Development of a
945 Neo-Epitope Specific Assay for Serological Assessment of Type VII Collagen Turnover and Its
946 Relevance in Fibroproliferative Disorders. Assay Drug Dev Technol. 2018;16(2):123–31. Epub
947 20180301. doi: 10.1089/adt.2017.820. PubMed PMID: 29493258.

948 54. Williams LM, McCann FE, Cabrita MA, Layton T, Cribbs A, Knezevic B, et al. Identifying
949 collagen VI as a target of fibrotic diseases regulated by CREBBP/EP300. Proc Natl Acad Sci U
950 S A. 2020;117(34):20753–63. Epub 2020/08/08. doi: 10.1073/pnas.2004281117. PubMed PMID:
951 32759223; PubMed Central PMCID: PMCPMC7456151.

55. Rehman S, Salway F, Stanley JK, Ollier WE, Day P, Bayat A. Molecular phenotypic descriptors of Dupuytren's disease defined using informatics analysis of the transcriptome. J Hand Surg Am. 2008;33(3):359–72. Epub 2008/03/18. doi: 10.1016/j.jhsa.2007.11.010. PubMed PMID: 18343292.

56. Vi L, Feng L, Zhu RD, Wu Y, Satish L, Gan BS, et al. Periostin differentially induces proliferation, contraction and apoptosis of primary Dupuytren's disease and adjacent palmar fascia cells. Exp Cell Res. 2009;315(20):3574–86. Epub 2009/07/22. doi: 10.1016/j.yexcr.2009.07.015. PubMed PMID: 19619531; PubMed Central PMCID: PMCPMC5017872.

57. Krause C, Kloen P, Ten Dijke P. Elevated transforming growth factor beta and mitogen-activated protein kinase pathways mediate fibrotic traits of Dupuytren's disease fibroblasts. Fibrogenesis Tissue Repair. 2011;4(1):14. Epub 2011/06/30. doi: 10.1186/1755-1536-4-14. PubMed PMID: 21711521; PubMed Central PMCID: PMCPMC3148569.

58. Forrester HB, Temple-Smith P, Ham S, de Kretser D, Southwick G, Sprung CN. Genome-wide analysis using exon arrays demonstrates an important role for expression of extra-cellular matrix, fibrotic control and tissue remodelling genes in Dupuytren's disease. PLoS One. 2013;8(3):e59056. Epub 2013/04/05. doi: 10.1371/journal.pone.0059056. PubMed PMID: 23554969; PubMed Central PMCID: PMCPMC3595223.

59. Ng M, Thakkar D, Southam L, Werker P, Ophoff R, Becker K, et al. A Genome-wide Association Study of Dupuytren Disease Reveals 17 Additional Variants Implicated in Fibrosis. Am J Hum Genet. 2017;101(3):417–27. Epub 2017/09/09. doi: 10.1016/j.ajhg.2017.08.006. PubMed PMID: 28886342; PubMed Central PMCID: PMCPMC5591021.

60. Park TH, Kim D, Lee YS, Kim SY. A meta-analysis to identify novel diagnostic and therapeutic targets for Dupuytren's disease. Wound Repair Regen. 2020;28(2):202–10. Epub 2019/11/07. doi: 10.1111/wrr.12774. PubMed PMID: 31688987.

61. Verjee LS, Verhoekx JS, Chan JK, Krausgruber T, Nicolaidou V, Izadi D, et al. Unraveling the signaling pathways promoting fibrosis in Dupuytren's disease reveals TNF as a therapeutic target. Proc Natl Acad Sci U S A. 2013;110(10):E928–37. Epub 2013/02/23. doi: 10.1073/pnas.1301100110. PubMed PMID: 23431165; PubMed Central PMCID: PMCPMC3593900.

62. Eaton C. Dupuytren Disease. In: Wolfe S, Pederson W, Kozin S, Cohen M, editors. Green's Operative Hand Surgery. 1. Eighth ed. Philadelphia: Elsevier; 2022. p. 148–81.

63. Akbar M, Garcia-Melchor E, Chilaka S, Little KJ, Sood S, Reilly JH, et al. Attenuation of Dupuytren's fibrosis via targeting of the STAT1 modulated IL-13Ralpha1 response. Sci Adv. 2020;6(28):eaaz8272. Epub 2020/07/23. doi: 10.1126/sciadv.aaz8272. PubMed PMID: 32695877; PubMed Central PMCID: PMCPMC7351483.

64. Kida H, Jiang JJ, Matsui Y, Takahashi I, Hasebe R, Kawamura D, et al. Dupuytren's contracture-associated SNPs increase SFRP4 expression in nonimmune cells including fibroblasts to enhance inflammation development. Int Immunol. 2023. Epub 20230131. doi: 10.1093/intimm/dxad004. PubMed PMID: 36719100.

65. Riesmeijer SA, Kamali Z, Ng M, Drichel D, Piersma B, Becker K, et al. A genome-wide association meta-analysis implicates Hedgehog and Notch signaling in Dupuytren's disease. Nat Commun. 2024;15(1):199. Epub 20240103. doi: 10.1038/s41467-023-44451-0. PubMed PMID: 38172110; PubMed Central PMCID: PMCPMC10764787.

66. Schultz HS, Nitze LM, Zeuthen LH, Keller P, Gruhler A, Pass J, et al. Collagen induces maturation of human monocyte-derived dendritic cells by signaling through osteoclast-

associated receptor. J Immunol. 2015;194(7):3169–79. Epub 20150227. doi: 10.4049/jimmunol.1402800. PubMed PMID: 25725106; PubMed Central PMCID: PMCPMC4367160.

67. Bakowska JC, Jupille H, Fatheddin P, Puertollano R, Blackstone C. Troyer syndrome protein spartin is mono-ubiquitinated and functions in EGF receptor trafficking. Mol Biol Cell. 2007;18(5):1683–92. Epub 20070301. doi: 10.1091/mbc.e06-09-0833. PubMed PMID: 17332501; PubMed Central PMCID: PMCPMC1855030.

68. Augoff K, Tabola R, Kula J, Gosk J, Rutowski R. Epidermal growth factor receptor (EGF-R) in Dupuytren's disease. J Hand Surg Br. 2005;30(6):570–3. Epub 2005/08/02. doi: 10.1016/j.jhsb.2005.06.008. PubMed PMID: 16055243.

69. Wang ML, Rajpar I, Ruggiero NA, Fertala J, Steplewski A, Beredjiklian PK, et al. Circulating inflammatory cytokines alter transcriptional activity within fibrotic tissue of Dupuytren's disease patients. J Orthop Res. 2021. Epub 2021/04/30. doi: 10.1002/jor.25059. PubMed PMID: 33913534.

70. Wilbrand S. Dupuytren´s Contracture : Features and Consequences. Uppsala: Acta Universitatis Upsaliensis; 2002.

71. Kuo RYL, Ng M, Prieto-Alhambra D, Furniss D. Dupuytren's Disease Predicts Increased All-Cause and Cancer-Specific Mortality: Analysis of a Large Cohort from the U.K. Clinical Practice Research Datalink. Plast Reconstr Surg. 2020;145(3):574e–82e. Epub 2020/02/26. doi: 10.1097/PRS.0000000000006551. PubMed PMID: 32097318; PubMed Central PMCID: PMCPMC7043723.

72. van Rijssen AL, ter Linden H, Werker PM. Five-year results of a randomized clinical trial on treatment in Dupuytren's disease: percutaneous needle fasciotomy versus limited

fasciectomy. Plast Reconstr Surg. 2012;129(2):469–77. Epub 2011/10/12. doi: 10.1097/PRS.0b013e31823aea95. PubMed PMID: 21987045.

73. Wilbrand S, Ekbom A, Gerdin B. The sex ratio and rate of reoperation for Dupuytren's contracture in men and women. J Hand Surg Br. 1999;24(4):456–9. Epub 1999/09/03. doi: 10.1054/jhsb.1999.0154. PubMed PMID: 10473157.

74. Kozanoglu E, Mete FS, Akalin BE, Aksoyler D, Berkoz O, Emekli U, et al. The epidemiological, etiological, and clinical comparisons of primary and recurrent Dupuytren's contractures. Ulus Travma Acil Cerrahi Derg. 2025;31(2):133–9. doi: 10.14744/tjtes.2024.95049. PubMed PMID: 39963920; PubMed Central PMCID: PMCPMC11843423.

75. Hauksson IT, Havdal MB, Benth JS, Hoelsbrekken SE, Randsborg PH. Collagenase Clostridium histolyticum Versus Needle Fasciotomy for Primary Metacarpophalangeal Dupuytren Contracture: Five-Year Results from a Randomized Controlled Trial. JB JS Open Access. 2024;9(4). Epub 20241120. doi: 10.2106/JBJS.OA.24.00038. PubMed PMID: 39569009; PubMed Central PMCID: PMCPMC11573333.

76. Karjalainen VL, Soikkeli J, Raisanen MP, Leppanen OV, Reito A, Stjernberg-Salmela S, et al. Progression of Dupuytren's contracture: a randomized controlled trial comparing surgery, needle fasciotomy, and collagenase injection. Plast Reconstr Surg. 2025. Epub 20251204. doi: 10.1097/PRS.0000000000012666. PubMed PMID: 41334972.

77. Raykha C, Crawford J, Gan BS, Fu P, Bach LA, O'Gorman DB. IGF-II and IGFBP-6 regulate cellular contractility and proliferation in Dupuytren's disease. Biochim Biophys Acta. 2013;1832(10):1511–9. Epub 2013/04/30. doi: 10.1016/j.bbadis.2013.04.018. PubMed PMID: 23623986.

78. O’Gorman DB. The Extracellular Matrix in Dupuytren Disease. Dupuytren Disease and Related Diseases - The Cutting Edge 2017. p. 43–54.

79. Pannecoeck R, Serruys D, Benmeridja L, Delanghe JR, van Geel N, Speeckaert R, et al. Vascular adhesion protein-1: Role in human pathology and application as a biomarker. Crit Rev Clin Lab Sci. 2015;52(6):284–300. Epub 20150818. doi: 10.3109/10408363.2015.1050714. PubMed PMID: 26287391.

80. Yepuri G, Velagapudi S, Xiong Y, Rajapakse AG, Montani JP, Ming XF, et al. Positive crosstalk between arginase-II and S6K1 in vascular endothelial inflammation and aging. Aging Cell. 2012;11(6):1005–16. Epub 20120918. doi: 10.1111/acel.12001. PubMed PMID: 22928666.

81. Volz J, Kusch C, Beck S, Popp M, Vogtle T, Meub M, et al. BIN2 orchestrates platelet calcium signaling in thrombosis and thrombo-inflammation. J Clin Invest. 2020;130(11):6064–79. doi: 10.1172/JCI136457. PubMed PMID: 32750041; PubMed Central PMCID: PMCPMC7598067.

82. Eaton C. The Next Stage of Clinical Dupuytren Research: Biomarkers and Chronic Disease Research Tools. In: al. PMNWe, editor. Dupuytren Disease and Related Diseases - The Cutting Edge. Switzerland: Springer; 2017. p. 391–407.

83. Yanase Y, Matsuo Y, Takahagi S, Kawaguchi T, Uchida K, Ishii K, et al. Coagulation factors induce human skin mast cell and basophil degranulation via activation of complement 5 and the C5a receptor. J Allergy Clin Immunol. 2021;147(3):1101–4 e7. Epub 20200902. doi: 10.1016/j.jaci.2020.08.018. PubMed PMID: 32888945.

84. Romejko K, Markowska M, Niemczyk S. The Review of Current Knowledge on Neutrophil Gelatinase-Associated Lipocalin (NGAL). Int J Mol Sci. 2023;24(13). Epub 20230621. doi: 10.3390/ijms241310470. PubMed PMID: 37445650; PubMed Central PMCID: PMCPMC10341718.

85. Verhoekx JS, Beckett KS, Bisson MA, McGrouther DA, Grobbelaar AO, Mudera V. The mechanical environment in Dupuytren's contracture determines cell contractility and associated

MMP-mediated matrix remodeling. J Orthop Res. 2013;31(2):328–34. Epub 2012/09/19. doi: 10.1002/jor.22220. PubMed PMID: 22987740.

86. Hammerman M, Blomgran P, Dansac A, Eliasson P, Aspenberg P. Different gene response to mechanical loading during early and late phases of rat Achilles tendon healing. J Appl Physiol (1985). 2017;123(4):800–15. Epub 20170713. doi: 10.1152/japplphysiol.00323.2017. PubMed PMID: 28705996.

87. Stocks M, Walter AS, Akova E, Gauglitz G, Aszodi A, Boecker W, et al. RNA-seq unravels distinct expression profiles of keloids and Dupuytren's disease. Heliyon. 2024;10(1):e23681. Epub 20231213. doi: 10.1016/j.heliyon.2023.e23681. PubMed PMID: 38187218; PubMed Central PMCID: PMCPMC10770622.

88. Wilutzky B, Berndt A, Katenkamp D, Koshmehl H. Programmed cell death in nodular palmar fibromatosis (Morbus Dupuytren). Histol Histopathol. 1998;13(1):67–72. Epub 1998/02/26. doi: 10.14670/HH-13.67. PubMed PMID: 9476635.

89. Tanaka T, Biancotto A, Moaddel R, Moore AZ, Gonzalez-Freire M, Aon MA, et al. Plasma proteomic signature of age in healthy humans. Aging Cell. 2018;17(5):e12799. Epub 2018/07/12. doi: 10.1111/acel.12799. PubMed PMID: 29992704; PubMed Central PMCID: PMCPMC6156492.

90. Park TJ, Curran T. Essential roles of Crk and CrkL in fibroblast structure and motility. Oncogene. 2014;33(43):5121–32. Epub 20131028. doi: 10.1038/onc.2013.453. PubMed PMID: 24166500.

91. Kanazawa T, Michida H, Uchino Y, Ishihara A, Zhang S, Tabata S, et al. Cell shape-based chemical screening reveals an epigenetic network mediated by focal adhesions. FEBS J. 2021;288(19):5613–28. Epub 20210422. doi: 10.1111/febs.15840. PubMed PMID: 33768715.

92. van Beuge MM, Ten Dam EJ, Werker PM, Bank RA. Wnt pathway in Dupuytren disease: connecting profibrotic signals. Transl Res. 2015;166(6):762–71 e3. Epub 2015/10/17. doi: 10.1016/j.trsl.2015.09.006. PubMed PMID: 26470681.

93. Satish L, LaFramboise WA, Johnson S, Vi L, Njarlangattil A, Raykha C, et al. Fibroblasts from phenotypically normal palmar fascia exhibit molecular profiles highly similar to fibroblasts from active disease in Dupuytren's Contracture. BMC Med Genomics. 2012;5:15. Epub 2012/05/09. doi: 10.1186/1755-8794-5-15. PubMed PMID: 22559715; PubMed Central PMCID: PMCPMC3375203.

94. Verhoekx JSN, Verjee LS, Izadi D, Chan JKK, Nicolaidou V, Davidson D, et al. Isometric contraction of Dupuytren's myofibroblasts is inhibited by blocking intercellular junctions. J Invest Dermatol. 2013;133(12):2664–71. Epub 2013/05/09. doi: 10.1038/jid.2013.219. PubMed PMID: 23652794.

95. Moch M, Schieren J, Leube RE. Cortical tension regulates desmosomal morphogenesis. Front Cell Dev Biol. 2022;10:946190. Epub 20221004. doi: 10.3389/fcell.2022.946190. PubMed PMID: 36268507; PubMed Central PMCID: PMCPMC9577410.

96. Ryu YH, Lee YJ, Kim KJ, Lee SJ, Han YN, Rhie JW. Epidermal Growth Factor (EGF)-Like Repeats and Discoidin I-Like Domains 3 (EDIL3): A Potential New Therapeutic Tool for the Treatment of Keloid Scars. Tissue Eng Regen Med. 2017;14(3):267–77. Epub 20170407. doi: 10.1007/s13770-017-0034-5. PubMed PMID: 30603483; PubMed Central PMCID: PMCPMC6171597.

97. Ferrero GB, Howald C, Micale L, Biamino E, Augello B, Fusco C, et al. An atypical 7q11.23 deletion in a normal IQ Williams-Beuren syndrome patient. Eur J Hum Genet. 2010;18(1):33–8. doi: 10.1038/ejhg.2009.108. PubMed PMID: 19568270; PubMed Central PMCID: PMCPMC2987159.

98. Millesi H, Reihsner R, Hamilton G, Mallinger R, Menzel EJ. Biomechanical properties of normal tendons, normal palmar aponeuroses and palmar aponeuroses from patients with Dupuytren's disease subjected to elastase and chondroitinase treatment. Connect Tissue Res. 1995;31(2):109–15. doi: 10.3109/03008209509028398. PubMed PMID: 15612326.

99. Deng L, Feng J, Broaddus RR. The novel estrogen-induced gene EIG121 regulates autophagy and promotes cell survival under stress. Cell Death Dis. 2010;1(4):e32. doi: 10.1038/cddis.2010.9. PubMed PMID: 21072319; PubMed Central PMCID: PMCPMC2976047.

100. Jemec B, Grobbelaar AO, Wilson GD, Smith PJ, Sanders R, McGrouther DA. Is Dupuytren's disease caused by an imbalance between proliferation and cell death? J Hand Surg Br. 1999;24(5):511–4. Epub 1999/12/22. doi: 10.1054/jhsb.1999.0251. PubMed PMID: 10597921.

101. Kaku M, Yamauchi M. Mechano-regulation of collagen biosynthesis in periodontal ligament. J Prosthodont Res. 2014;58(4):193–207. Epub 2014/10/15. doi: 10.1016/j.jpor.2014.08.003. PubMed PMID: 25311991; PubMed Central PMCID: PMCPMC4253671.

102. Li T, Qiu J, Jia T, Liang Y, Zhang K, Yan W, et al. G3BP2 regulates oscillatory shear stress-induced endothelial dysfunction. Genes Dis. 2022;9(6):1701–15. Epub 20211119. doi: 10.1016/j.gendis.2021.11.003. PubMed PMID: 36157502; PubMed Central PMCID: PMCPMC9485288.

103. Wei SC, Fattet L, Tsai JH, Guo Y, Pai VH, Majeski HE, et al. Matrix stiffness drives epithelial-mesenchymal transition and tumour metastasis through a TWIST1-G3BP2 mechanotransduction pathway. Nat Cell Biol. 2015;17(5):678–88. Epub 20150420. doi: 10.1038/ncb3157. PubMed PMID: 25893917; PubMed Central PMCID: PMCPMC4452027.

104. Modjeski KL, Ture SK, Field DJ, Cameron SJ, Morrell CN. Glutamate Receptor Interacting Protein 1 Mediates Platelet Adhesion and Thrombus Formation. PLoS One. 2016;11(9):e0160638. Epub 20160915. doi: 10.1371/journal.pone.0160638. PubMed PMID: 27631377; PubMed Central PMCID: PMCPMC5025166.

105. Tomatsu S, Montano AM, Dung VC, Grubb JH, Sly WS. Mutations and polymorphisms in GUSB gene in mucopolysaccharidosis VII (Sly Syndrome). Hum Mutat. 2009;30(4):511–9. doi: 10.1002/humu.20828. PubMed PMID: 19224584; PubMed Central PMCID: PMCPMC3048808.

106. Chakraborty A, Edkins AL. HSP90 as a regulator of extracellular matrix dynamics. Biochem Soc Trans. 2021;49(6):2611–25. doi: 10.1042/BST20210374. PubMed PMID: 34913470.

107. de la Mare JA, Jurgens T, Edkins AL. Extracellular Hsp90 and TGFbeta regulate adhesion, migration and anchorage independent growth in a paired colon cancer cell line model. BMC Cancer. 2017;17(1):202. Epub 20170316. doi: 10.1186/s12885-017-3190-z. PubMed PMID: 28302086; PubMed Central PMCID: PMCPMC5356307.

108. Terzuoli E, Corti F, Nannelli G, Giachetti A, Donnini S, Ziche M. Bradykinin B2 Receptor Contributes to Inflammatory Responses in Human Endothelial Cells by the Transactivation of the Fibroblast Growth Factor Receptor FGFR-1. Int J Mol Sci. 2018;19(9). Epub 20180906. doi: 10.3390/ijms19092638. PubMed PMID: 30200598; PubMed Central PMCID: PMCPMC6163484.

109. Vandersleyen V, Grosber M, Wilgenhof S, De Kock J, Neyns B, Gutermuth J. Vemurafenib-associated Dupuytren- and Ledderhose palmoplantar fibromatosis in metastatic melanoma patients. J Eur Acad Dermatol Venereol. 2016;30(7):1133–5. Epub 20150824. doi: 10.1111/jdv.13268. PubMed PMID: 26303964.

110. Higuchi Y, Ogata T, Nakanishi N, Nishi M, Tsuji Y, Tomita S, et al. Cavin-2 promotes fibroblast-to-myofibroblast trans-differentiation and aggravates cardiac fibrosis. ESC Heart Fail. 2023. Epub 20231024. doi: 10.1002/ehf2.14571. PubMed PMID: 37872863.

111. Gokel JM, Hübner G. Occurrence of Myofibroblasts in the Different Phases of Morbus Dupuytren (Dupuytren's Contracture). Beiträge zur Pathologie. 1977;161(2):166–75. doi: 10.1016/s0005-8165(77)80095-4.

112. Chothani S, Schafer S, Adami E, Viswanathan S, Widjaja AA, Langley SR, et al. Widespread Translational Control of Fibrosis in the Human Heart by RNA-Binding Proteins. Circulation. 2019;140(11):937–51. Epub 20190709. doi: 10.1161/CIRCULATIONAHA.119.039596. PubMed PMID: 31284728; PubMed Central PMCID: PMCPMC6749977.

113. Drazic A, Aksnes H, Marie M, Boczkowska M, Varland S, Timmerman E, et al. NAA80 is actin's N-terminal acetyltransferase and regulates cytoskeleton assembly and cell motility. Proc Natl Acad Sci U S A. 2018;115(17):4399–404. Epub 20180326. doi: 10.1073/pnas.1718336115. PubMed PMID: 29581253; PubMed Central PMCID: PMCPMC5924898.

114. Bergenudd H, LindgÄRde F, Nilsson BE. Prevalence of Dupuytren’s Contracture and its Correlation with Degenerative Changes of the Hands and Feet and with Criteria of General Health. Journal of Hand Surgery. 2016;18(2):254–7. doi: 10.1016/0266-7681(93)90123-w.

115. Flint MH. The genesis of the palmar lesion. In: McFarlane RM, McGrouther DA, Flint MH, editors. Dupuytren's Disease Biology and Treatment. Edinburg Churchill Livingstone; 1990.

116. Worku MG, Seretew WS, Angaw DA, Tesema GA. Prevalence and Associated Factor of Brown Adipose Tissue: Systematic Review and Meta-Analysis. Biomed Res Int. 2020;2020:9106976. Epub 20200616. doi: 10.1155/2020/9106976. PubMed PMID: 32685543; PubMed Central PMCID: PMCPMC7317326.

117. Hamamoto H, Ueba Y, Sudo Y, Sanada H, Yamamuro T, Takeda T. Dupuytren's contracture: morphological and biochemical changes in palmar aponeurosis. Hand. 1982;14(3):237–47. Epub 1982/10/01. doi: 10.1016/s0072-968x(82)80056-9. PubMed PMID: 6130030.

118. Shih B, Brown JJ, Armstrong DJ, Lindau T, Bayat A. Differential gene expression analysis of subcutaneous fat, fascia, and skin overlying a Dupuytren's disease nodule in comparison to control tissue. Hand (N Y). 2009;4(3):294–301. Epub 2009/02/03. doi: 10.1007/s11552-009-9164-0. PubMed PMID: 19184239; PubMed Central PMCID: PMCPMC2724615.

119. Tripkovic I, Ogorevc M, Vukovic D, Saraga-Babic M, Mardesic S. Fibrosis-Associated Signaling Molecules Are Differentially Expressed in Palmar Connective Tissues of Patients with Carpal Tunnel Syndrome and Dupuytren's Disease. Biomedicines. 2022;10(12). Epub 20221211. doi: 10.3390/biomedicines10123214. PubMed PMID: 36551969; PubMed Central PMCID: PMCPMC9775445.

120. Docheva D, Vaerst B, Deiler S, Giunta RE, Schieker M, Volkmer E. [Alterations of cell phenotype in Dupuytren's disease--an in vitro analysis]. Handchir Mikrochir Plast Chir. 2012;44(2):59–66. Epub 2012/04/13. doi: 10.1055/s-0032-1309025. PubMed PMID: 22495955.

121. Devine MJ, Birsa N, Kittler JT. Miro sculpts mitochondrial dynamics in neuronal health and disease. Neurobiol Dis. 2016;90:27–34. Epub 20151219. doi: 10.1016/j.nbd.2015.12.008. PubMed PMID: 26707701.

122. Garcia-Martinez I, Garcia-Mesa Y, Garcia-Piqueras J, Martinez-Pubil A, Cobo JL, Feito J, et al. Sensory innervation of the human palmar aponeurosis in healthy individuals and patients with palmar fibromatosis. J Anat. 2021. Epub 20211208. doi: 10.1111/joa.13609. PubMed PMID: 34881452.

123. Nanchahal J, Chan JK. Treatments for early-stage Dupuytren's disease: an evidence-based approach. J Hand Surg Eur Vol. 2023:17531934221131373. Epub 20230113. doi: 10.1177/17531934221131373. PubMed PMID: 36638105.

124. Joshi H, Morley SC. Cells under stress: The mechanical environment shapes inflammasome responses to danger signals. J Leukoc Biol. 2019;106(1):119–25. Epub 20190115. doi: 10.1002/JLB.3MIR1118-417R. PubMed PMID: 30645000; PubMed Central PMCID: PMCPMC6784827.

125. Ali MK, Kim RY, Brown AC, Donovan C, Vanka KS, Mayall JR, et al. Critical role for iron accumulation in the pathogenesis of fibrotic lung disease. J Pathol. 2020;251(1):49–62. Epub 20200330. doi: 10.1002/path.5401. PubMed PMID: 32083318.

126. Ushijima M, Tsuneyoshi M, Enjoji M. Dupuytren type fibromatoses. A clinicopathologic study of 62 cases. Acta Pathol Jpn. 1984;34(5):991–1001. Epub 1984/09/01. doi: 10.1111/j.1440-1827.1984.tb07630.x. PubMed PMID: 6507097.

127. Verjee LS, Midwood K, Davidson D, Essex D, Sandison A, Nanchahal J. Myofibroblast distribution in Dupuytren's cords: correlation with digital contracture. J Hand Surg Am. 2009;34(10):1785–94. Epub 2009/11/17. doi: 10.1016/j.jhsa.2009.08.005. PubMed PMID: 19910144.

128. Kischer CW, Speer DP. Microvascular changes in Dupuytren's contracture. J Hand Surg Am. 1984;9A(1):58–62. doi: 10.1016/s0363-5023(84)80185-9. PubMed PMID: 6693745.

129. Aarabi S, Bhatt KA, Shi Y, Paterno J, Chang EI, Loh SA, et al. Mechanical load initiates hypertrophic scar formation through decreased cellular apoptosis. FASEB J. 2007;21(12):3250–61. Epub 2007/05/17. doi: 10.1096/fj.07-8218com. PubMed PMID: 17504973.

130. Sood RF, Hocking AM, Muffley LA, Ga M, Honari S, Reiner AP, et al. Genome-wide Association Study of Postburn Scarring Identifies a Novel Protective Variant. Ann Surg. 2015;262(4):563–9. doi: 10.1097/SLA.0000000000001439. PubMed PMID: 26366535; PubMed Central PMCID: PMCPMC9632222.

131. Viji Babu PK, Rianna C, Belge G, Mirastschijski U, Radmacher M. Mechanical and migratory properties of normal, scar, and Dupuytren's fibroblasts. J Mol Recognit. 2018;31(9):e2719. Epub 2018/04/28. doi: 10.1002/jmr.2719. PubMed PMID: 29701269.

132. Teckchandani A, Toida N, Goodchild J, Henderson C, Watts J, Wollscheid B, et al. Quantitative proteomics identifies a Dab2/integrin module regulating cell migration. J Cell Biol. 2009;186(1):99–111. Epub 20090706. doi: 10.1083/jcb.200812160. PubMed PMID: 19581412; PubMed Central PMCID: PMCPMC2712992.

133. Johnston P, Chojnowski AJ, Davidson RK, Riley GP, Donell ST, Clark IM. A complete expression profile of matrix-degrading metalloproteinases in Dupuytren's disease. J Hand Surg Am. 2007;32(3):343–51. Epub 2007/03/06. doi: 10.1016/j.jhsa.2006.12.010. PubMed PMID: 17336841.

134. D'Amico F, Candido S, Libra M. Interaction between matrix metalloproteinase-9 (MMP-9) and neutrophil gelatinase-associated lipocalin (NGAL): A recent evolutionary event in primates. Dev Comp Immunol. 2021;116:103933. Epub 20201124. doi: 10.1016/j.dci.2020.103933. PubMed PMID: 33245981.

135. Luo L, Deng L, Chen Y, Ding R, Li X. Identification of Lipocalin 2 as a Ferroptosis-Related Key Gene Associated with Hypoxic-Ischemic Brain Damage via STAT3/NF-kappaB Signaling Pathway. Antioxidants (Basel). 2023;12(1). Epub 20230112. doi: 10.3390/antiox12010186. PubMed PMID: 36671050; PubMed Central PMCID: PMCPMC9854551.

136. Wipff PJ, Hinz B. Integrins and the activation of latent transforming growth factor beta1 - an intimate relationship. Eur J Cell Biol. 2008;87(8-9):601–15. Epub 2008/03/18. doi: 10.1016/j.ejcb.2008.01.012. PubMed PMID: 18342983.

137. Dong G, Huang X, Jiang S, Ni L, Chen S. Simvastatin Mitigates Apoptosis and Transforming Growth Factor-Beta Upregulation in Stretch-Induced Endothelial Cells. Oxid Med Cell Longev. 2019;2019:6026051. Epub 20191217. doi: 10.1155/2019/6026051. PubMed PMID: 31934265; PubMed Central PMCID: PMCPMC6942893.

138. Lyons RM, Gentry LE, Purchio AF, Moses HL. Mechanism of activation of latent recombinant transforming growth factor beta 1 by plasmin. J Cell Biol. 1990;110(4):1361–7. doi: 10.1083/jcb.110.4.1361. PubMed PMID: 2139036; PubMed Central PMCID: PMCPMC2116088.

139. Flevaris P, Vaughan D. The Role of Plasminogen Activator Inhibitor Type-1 in Fibrosis. Semin Thromb Hemost. 2017;43(2):169–77. Epub 20160824. doi: 10.1055/s-0036-1586228. PubMed PMID: 27556351.

140. Howard JC, Varallo VM, Ross DC, Faber KJ, Roth JH, Seney S, et al. Wound healing-associated proteins Hsp47 and fibronectin are elevated in Dupuytren's contracture. J Surg Res. 2004;117(2):232–8. Epub 2004/03/30. doi: 10.1016/j.jss.2004.01.013. PubMed PMID: 15047128.

141. Hosokawa N, Hohenadl C, Satoh M, Kuhn K, Nagata K. HSP47, a collagen-specific molecular chaperone, delays the secretion of type III procollagen transfected in human embryonic kidney cell line 293: a possible role for HSP47 in collagen modification. J Biochem. 1998;124(3):654–62. doi: 10.1093/oxfordjournals.jbchem.a022162. PubMed PMID: 9722680.

142. Li Z, Ivanov AA, Su R, Gonzalez-Pecchi V, Qi Q, Liu S, et al. The OncoPPi network of cancer-focused protein-protein interactions to inform biological insights and therapeutic

strategies. Nat Commun. 2017;8:14356. Epub 20170216. doi: 10.1038/ncomms14356. PubMed PMID: 28205554; PubMed Central PMCID: PMCPMC5316855.

143. van den Broek LJ, van der Veer WM, de Jong EH, Gibbs S, Niessen FB. Suppressed inflammatory gene expression during human hypertrophic scar compared to normotrophic scar formation. Exp Dermatol. 2015;24(8):623–9. Epub 20150526. doi: 10.1111/exd.12739. PubMed PMID: 25939875.

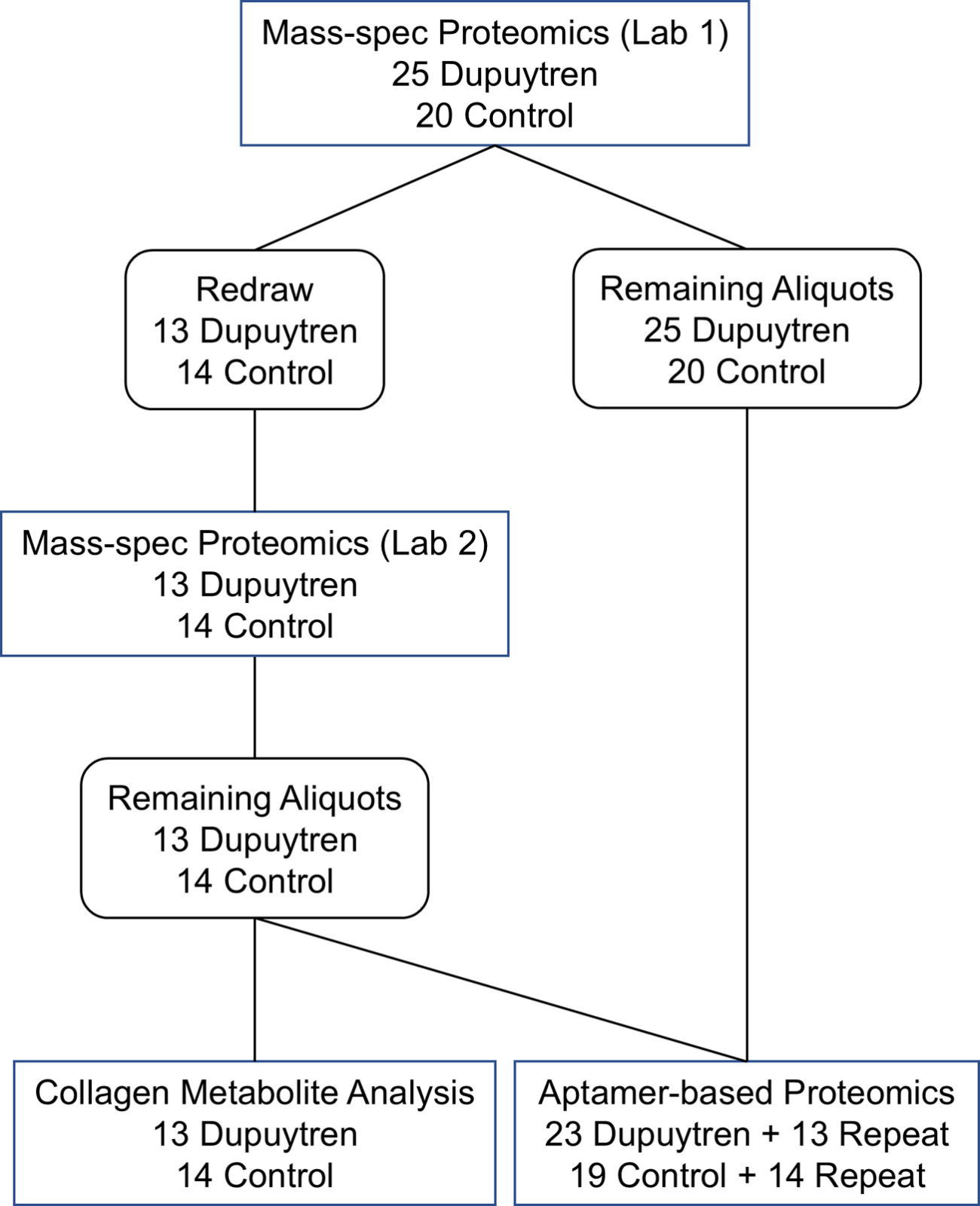
Mass-spec Proteomics (Lab 1)
25 Dupuytren
20 Control
Redraw
13 Dupuytren
14 Control
Remaining Aliquots
25 Dupuytren
20 Control
Mass-spec Proteomics (Lab 2)
13 Dupuytren
14 Control
Remaining Aliquots
13 Dupuytren
14 Control
Collagen Metabolite Analysis
13 Dupuytren
14 Control
Aptamer-based Proteomics
23 Dupuytren + 13 Repeat
19 Control + 14 Repeat

	C&C	ECM	ENZ	MBR	PPL	SGN
ACAN		■				
AKR1A1		■				
BIN2		■				
C5	■	■	■			■
C6	■	■				
CALCB		■				■
CASP3			■			■
CGA		■				■
CGB3		■				
CGB7		■				
CPB1		■				
CRKL				■	■	■
CSNK1G2						■
DSG2		■				■
EDIL3		■				
FKBP5		■				■
GUSB		■				
HGS		■				■
HSP90AA1						■
KNG1	■		■			■
MAP3K11						■
NRG4						■
PCSK9				■		
PRKAR2B			■			■
RHOT1						■
SERPINC1	■		■			
SOCS3			■		■	
SYK				■	■	
TF				■		
USP8				■		
WFIKKN2			■			
YWHAB			■		■	

	CAN	C&C	ECM	INL	INF	MBR	MFB	PPL	SGN	WNT
ACAN			■							
CASP3	■		■	■	■		■	■	■	
COL1A1	■	■	■		■	■	■	■	■	■
CSNK1G2								■		■
DAB2							■	■		■
DDR2			■			■	■	■		
HPX			■					■	■	
KNG1	■	■	■		■		■			
LCN2				■						
MAP2K1	■		■	■	■	■	■	■	■	
PLAT	■	■					■	■	■	
POSTN			■							
PRKCA	■	■	■		■	■	■	■	■	■
SERPINH1			■							
SFRP4							■			■
SMAD1							■	■		
STAT1	■		■	■	■	■	■	■	■	
STAT3	■		■	■	■	■	■	■	■	
TF	■	■					■	■		
USP8							■	■		■
YWHAZ	■	■		■	■		■	■		■

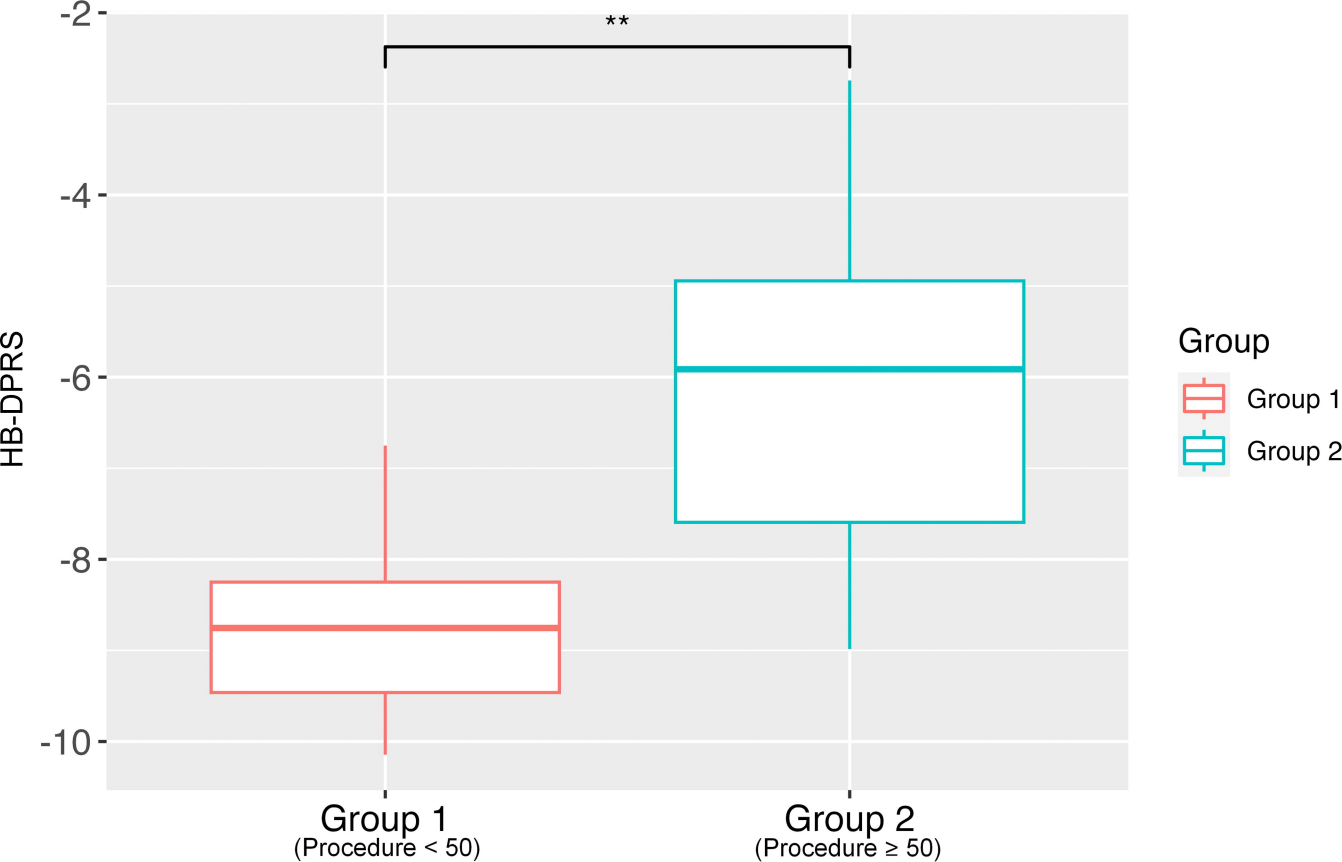
**
-2
-4
-6
-8
-10
HB-DPRS
Group 1
(Procedure < 50)
Group 2
(Procedure ≥ 50)
Group
Group 1
Group 2

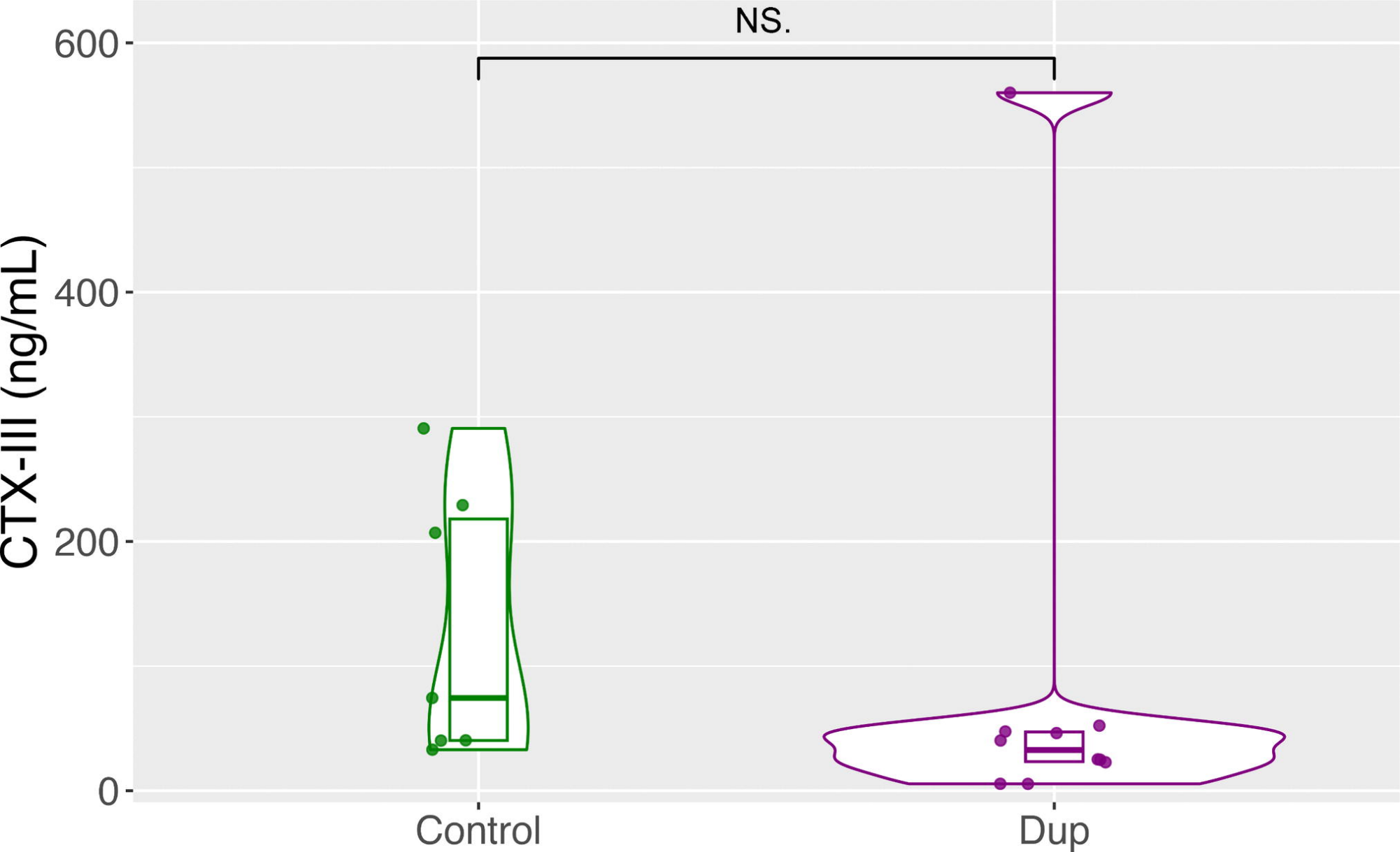
NS.
600
400
200
0
CTX-III (ng/mL)
Control
Dup

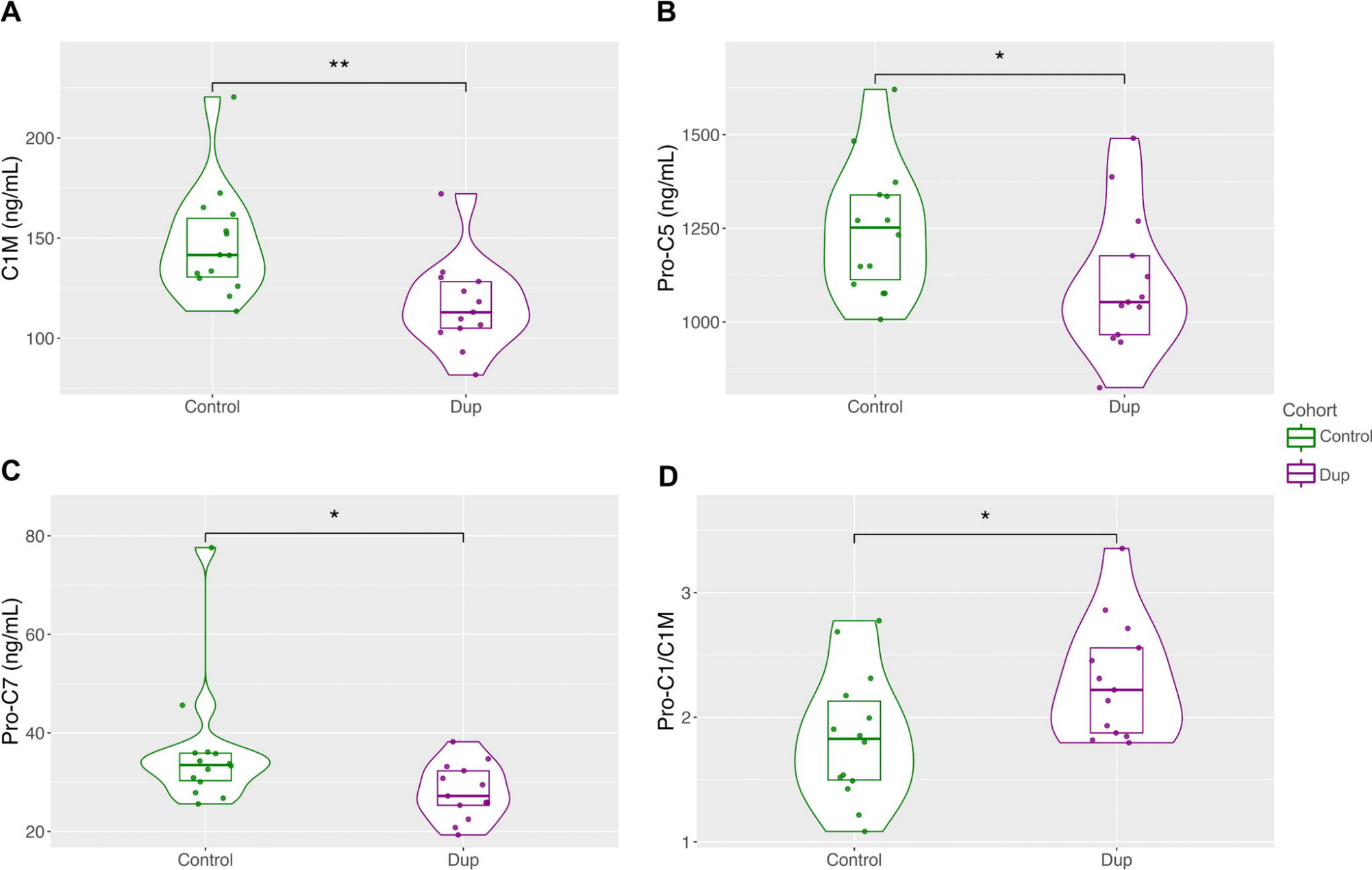
A
**
C1M (ng/mL)
200
150
100
Control
Dup
B
*
Pro-C5 (ng/mL)
1500
1250
1000
Control
Dup
Cohort
Control
Dup
C
*
Pro-C7 (ng/mL)
80
60
40
20
Control
Dup
D
*
Pro-C1/C1M
3
2
1
Control
Dup

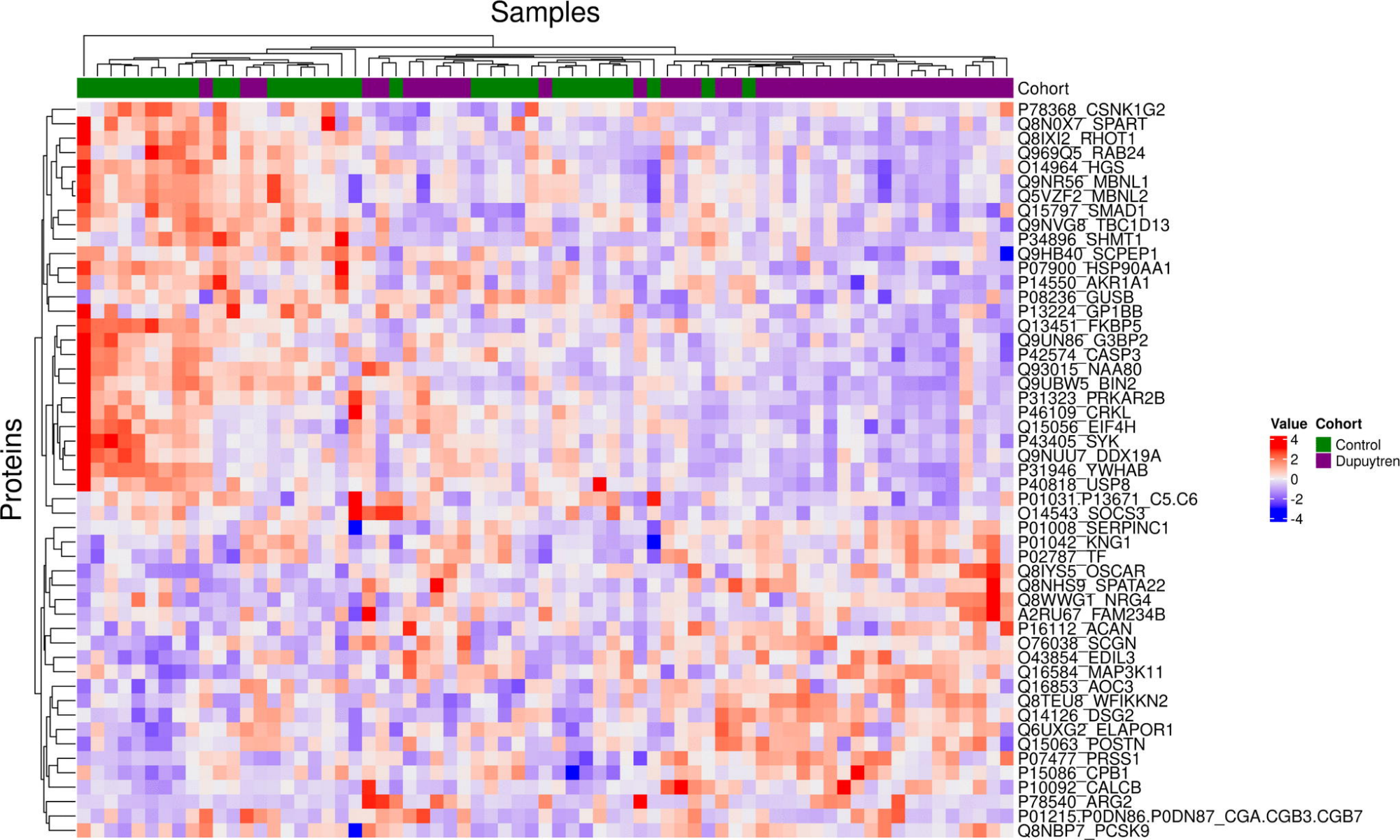
Samples
Cohort
Proteins
P78368_CSNK1G2
Q8N0X7_SPART
Q8IXI2_RHOT1
Q969Q5_RAB24
O14964_HGS
Q9NR56_MBNL1
Q5VZF2_MBNL2
Q15797_SMAD1
Q9NVG8_TBC1D13
P34896_SHMT1
Q9HB40_SCPEP1
P07900_HSP90AA1
P14550_AKR1A1
P08236_GUSB
P13224_GP1BB
Q13451_FKBP5
Q9UN86_G3BP2
P42574_CASP3
Q93015_NAA80
Q9UBW5_BIN2
P31323_PRKAR2B
P46109_CRKL
Q15056_EIF4H
P43405_SYK
Q9NUU7_DDX19A
P31946_YWHAB
P40818_USP8
P01031.P13671_C5.C6
O14543_SOCS3
P01008_SERPINC1
P01042_KNG1
P02787_TF
Q8IYS5_OSCAR
Q8NHS9_SPATA22
Q8WWG1_NRG4
A2RU67_FAM234B
P16112_ACAN
O76038_SCGN
O43854_EDIL3
Q16584_MAP3K11
Q16853_AOC3
Q8TEU8_WFIKKN2
Q14126_DSG2
Q6UXG2_ELAPOR1
Q15063_POSTN
P07477_PRSS1
P15086_CPB1
P10092_CALCB
P78540_ARG2
P01215.P0DN86.P0DN87_CGA.CGB3.CGB7
Q8NBP7_PCSK9
Value
4
2
0
-2
-4
Cohort
Control
Dupuytren

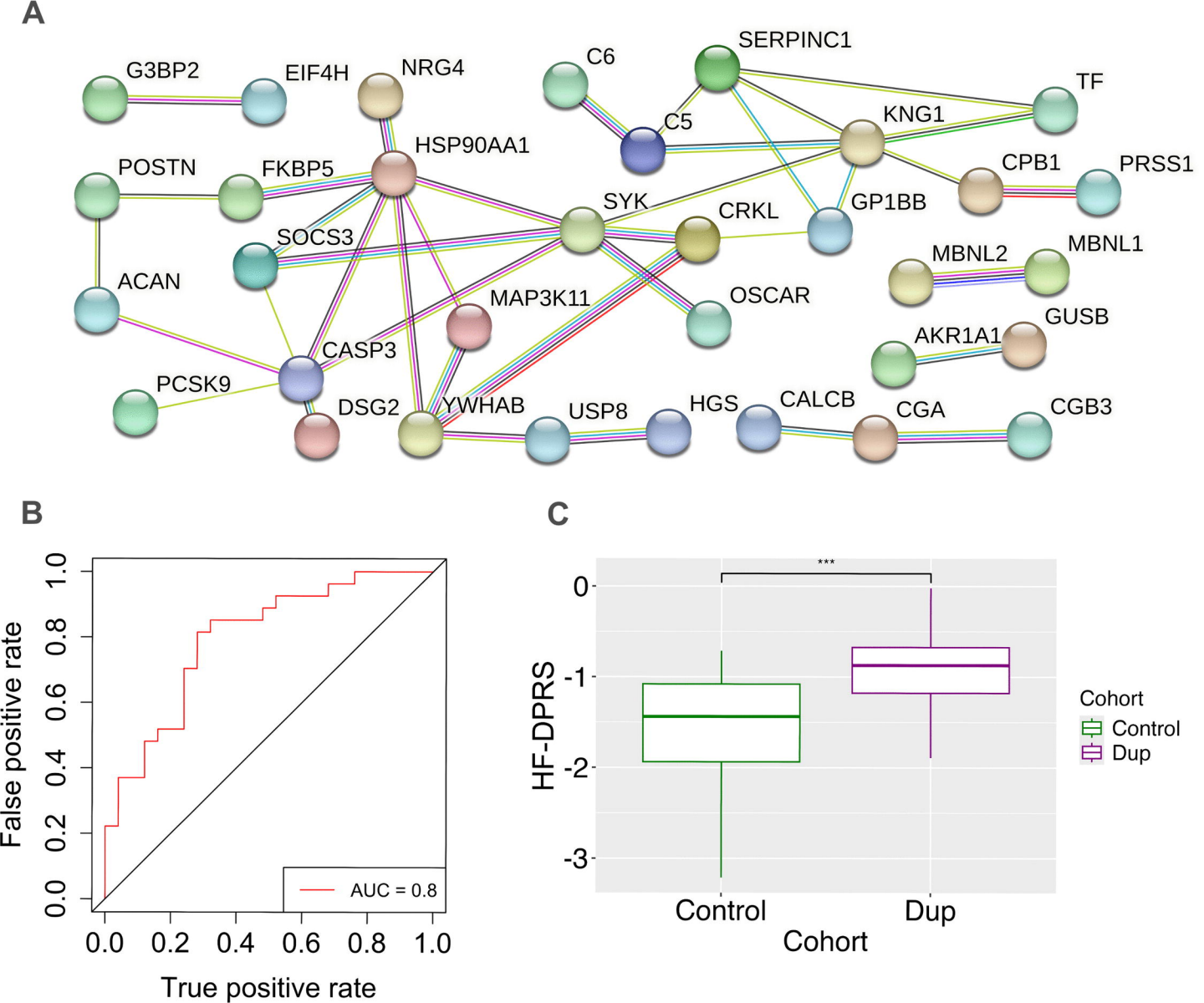
A
G3BP2
EIF4H
NRG4
C6
SERPINC1
TF
C5
KNG1
HSP90AA1
POSTN
FKBP5
CPB1
PRSS1
SYK
CRKL
GP1BB
SOCS3
MBNL2
MBNL1
ACAN
MAP3K11
OSCAR
GUSB
AKR1A1
CASP3
PCSK9
DSG2
YWHAB
USP8
HGS
CALCB
CGA
CGB3
B
False positive rate
True positive rate
0.0
0.2
0.4
0.6
0.8
1.0
AUC = 0.8
C
HF-DPRS
0
-1
-2
-3
***
Control
Dup
Cohort
Cohort
Control
Dup

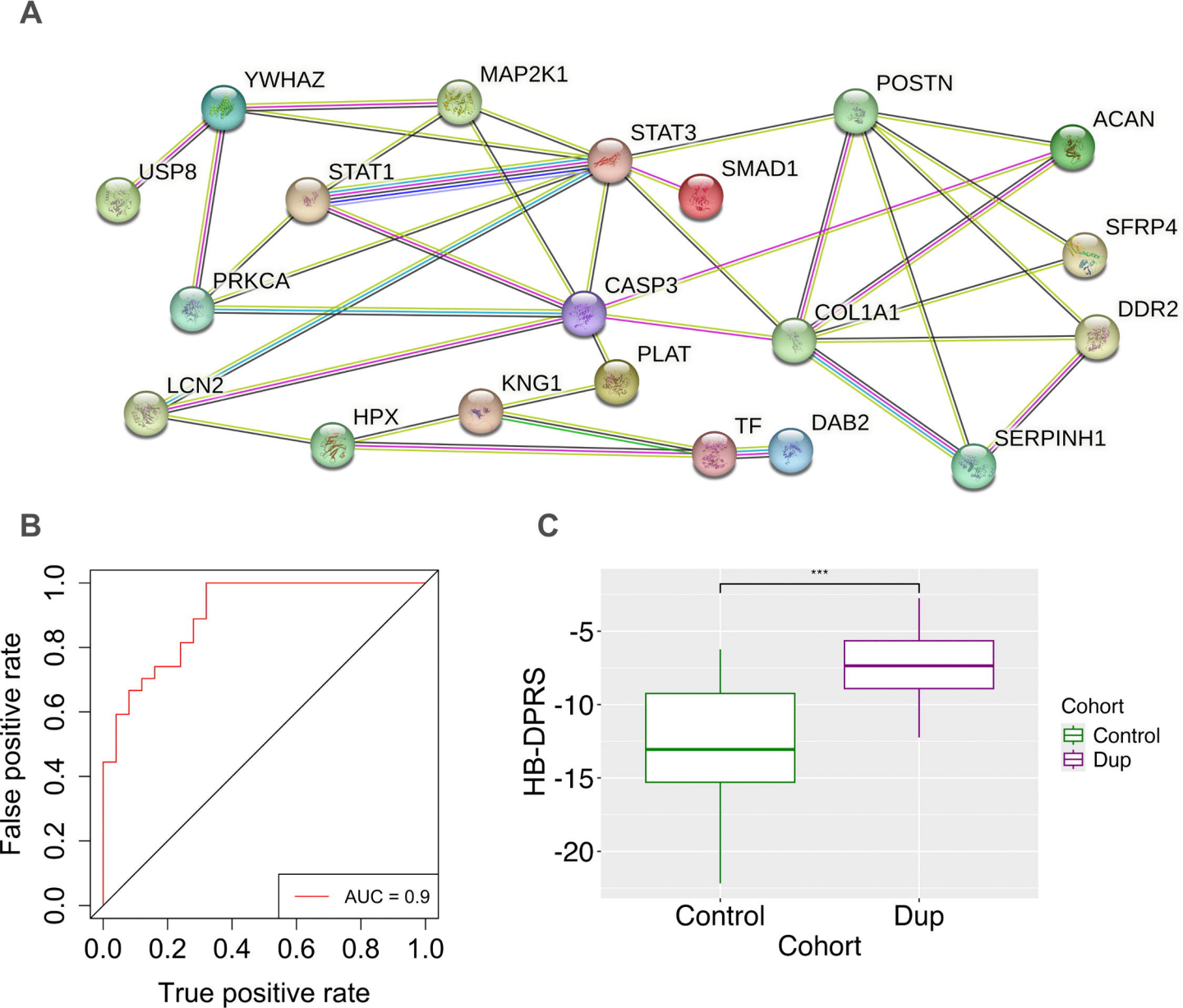
A
YWHAZ
MAP2K1
POSTN
ACAN
STAT3
USP8
STAT1
SMAD1
SFRP4
PRKCA
CASP3
COL1A1
DDR2
PLAT
LCN2
KNG1
HPX
TF
DAB2
SERPINH1
B
False positive rate
True positive rate
0.0
0.2
0.4
0.6
0.8
1.0
AUC = 0.9
C
***
HB-DPRS
-5
-10
-15
-20
Control
Dup
Cohort
Cohort
Control
Dup